Adaptive potential in the face of a transmissible cancer in Tasmanian devils

Kasha Strickland[1*], Menna E. Jones[2], Andrew Storfer[3], Rodrigo K Hamede[2], Paul A Hohenlohe[4], Mark J Margres[5], Hamish I McCallum[6], Sebastien Comte[7], Shelly Lachish[8], Loeske E B Kruuk[1]

1. Institute of Ecology and Evolution, School of Biological Sciences, University of Edinburgh, UK
2. School of Natural Sciences, University of Tasmania, Hobart, TAS, Australia
3. School of Biological Sciences, Washington State University, Pullman, Washington, USA 99164-4236
4. Department of Biological Sciences, University of Idaho, Moscow, Idaho 83844
5. Department of Integrative Biology, University of South Florida, Tampa, FL, USA
6. Environmental Futures Research Institute, Griffith University, Nathan, Queensland, Australia
7. Vertebrate Pest Research Unit, NSW Department of Primary Industries, 1447 Forest Rd, Orange NSW 2800, Australia
8. Public Health Intelligence Branch, Queensland Public Health and Scientific Services Division, Queensland Health, 15 Butterfield Street, Herston, QLD 4006

* corresponding author: kasha.strickland@ed.ac.uk

Abstract

Emerging infectious diseases (EIDs) cause catastrophic declines in wildlife populations, but also generate selective pressures that may result in rapid evolutionary responses. One such EID is devil facial tumour disease (DFTD) in the Tasmanian devil. DFTD is almost always fatal, which likely causes strong selection for traits that reduce susceptibility to the disease, but population decline has also left Tasmanian devils vulnerable to inbreeding depression. We analysed 22 years of data from an ongoing study of a population of Tasmanian devils on Freycinet Peninsula, Tasmania, to (1) identify whether DFTD may be causing selection on body size, by estimating phenotypic and genetic correlations between DFTD and size traits, (2) estimate the additive genetic variance of susceptibility to DFTD, and (3) investigate whether size traits or susceptibility to DFTD were under inbreeding depression. We found a positive phenotypic relationship between head width and susceptibility to DFTD, but this was not underpinned by a genetic correlation. Conversely, we found a negative phenotypic relationship between body weight and susceptibility to DFTD, and there was evidence for a negative genetic correlation between susceptibility to DFTD and body weight. There was additive genetic variance in susceptibility to DFTD, head width and body weight, but there was no evidence for inbreeding depression in any of these traits. These results suggest Tasmanian devils have the potential to respond adaptively to DFTD, although the realised evolutionary response will critically depend on the evolution of DFTD itself.

Keywords: transmissible cancer, wildlife disease, quantitative genetics, selection differential, adaptive potential, inbreeding depression

Introduction

Emerging infectious diseases (EIDs) are often critical drivers of population and evolutionary dynamics in their host species (Daszak et al., 2000; Schrag & Wiener, 1995). In particular, EIDs can induce rapid evolutionary responses in traits that determine hosts' exposure to pathogens (Herrera & Nunn, 2019), pathogen load (disease resistance/susceptibility; (Rigby et al., 2002)) and/or the costs of infection (disease tolerance; (Medzhitov et al., 2012)), especially in cases where EIDs impact fertility or cause rapid mortality (Altizer et al., 2003; Cunningham et al., 2021). However, whilst the ecological impacts of EIDs in natural populations are widely reported, including rapid population decline and species range contractions (Fisher & Garner, 2020; C. Hoffmann et al., 2017; Hoyt et al., 2021), empirical evidence for evolutionary consequences of the emergence of infectious diseases in wild populations has been more limited, likely due to a lack of appropriate individual-based data.

EIDs should select for traits which improve host immune defences (Hayward et al., 2014; Rarberg & Stjernman, 2003), but an adaptive evolutionary response in the susceptibility to disease is dependent on there being standing genetic variation in immune related traits (A. A. Hoffmann et al., 2017). In wild populations, genetic variation in traits can be estimated by combining individual-level phenotypic data with either a pedigree or genomic relatedness data (Wilson et al., 2010), and although these data are hard to collect in natural populations, some recent studies have used data from long-term field projects to estimate genetic variance in susceptibility to disease. These studies have reported a range of estimates of genetic variance, from a heritability of 0.12 for *Mycobacterium bovis* infection in European badgers (Marjamäki et al., 2021) and 0.13 for *Chlamydia pecorum* infection in koalas (Cristescu et al., 2022), to a relatively high heritability of 0.55 for *Mycoplasma ovipneumoniae* infection in bighorn sheep (Martin et al., 2021). Despite these recent studies, however, estimates of genetic variation in susceptibility to pathogens in wild populations remain rare, limiting our understanding of the potential for adaptive responses to EIDs in the wild.

Selection caused by EIDs should also indirectly impact traits that are correlated with individuals' susceptibility to the disease. Body size, for instance, is an important fitness-related trait that shapes individual variation in life-history traits (Healy et al., 2019) and is likely correlated with disease traits as a result of trade-offs caused by differential allocation of resources (Coltman et al., 2001; Gleeson et al., 2005; Silk & Hodgson, 2021; Valenzuela-Sánchez et al., 2021). A response to disease-induced selection in size traits would require a

genetic correlation between size and susceptibility to disease. However, phenotypic correlations may also be driven by components of the environment that simultaneously impact both traits, which may not result in evolutionary change (Falconer & Mackay, 1996). As such, identifying whether phenotypic relationships are caused by genetic covariances is important in predicting the observed response to selection in either trait (Lande & Arnold, 1983).

Whilst EIDs may induce selection for immune traits and those genetically correlated with them, population declines following the emergence of disease can also cause a rapid decline in genetic diversity concurrent with an increase in inbreeding (Hedrick & Kalinowski, 2000). Increased inbreeding causes increased genome-wide homozygosity and, where this directly impacts fitness, will result in inbreeding depression (i.e., reduced fitness caused by inbreeding) (O'Grady et al., 2006). Due to the tight association between disease traits and fitness components (i.e., survival and/or reproduction), immune traits are likely to be depressed under increased inbreeding (Spielman et al., 2004), which has been documented in a number of wild animals (e.g. Reid et al., 2003; Ross-Gillespie et al., 2007; Trinkel et al., 2011). When assessing the evolutionary impact of EIDs in declining populations, it is therefore necessary to test for inbreeding depression in immune-related traits.

An EID currently imposing extreme selection in a wild animal population is the transmissible cancer, devil facial tumour disease (DFTD), in Tasmanian Devils (*Sarcophilus harrisii*). Tasmanian devils are the largest extant carnivorous marsupial, and are endemic to the island of Tasmania, Australia. DFTD is a transmissible cancer that originated in a single Schwann cell in the 1980s (Murchison et al., 2010; Patton et al., 2020), and has since spread across almost the entirety of the species' range (Cunningham et al., 2021). Tumour cells are transmitted between hosts by allograft, often during aggressive interactions in the mating season or in competitive carrion feeding interactions when biting occurs (Hamede et al., 2013). With very few exceptions (Pye et al., 2016), DFTD evades an immune response, becomes malignant and causes mortality within 6 - 9 months of symptom onset (McCallum, 2008). As a result, DFTD has caused local population declines of over 80% (Cunningham et al., 2021; McCallum et al., 2007). Given the near 100% mortality associated with DFTD once infected, it is likely that the emergence of the disease has generated strong selection for traits that reduce susceptibility to the disease, and hence also on any genetically correlated traits. Accordingly, several studies have provided evidence for phenotypic and genomic changes in devil populations since the arrival of DFTD. First, allele frequencies at some immune-function genes

have changed since DFTD emerged, indicating that there might be contemporary selection on immunity (Epstein et al., 2016; Stahlke et al., 2021). Second, the rate of females breeding at one year's old increased sharply after DFTD was first detected (Jones et al., 2008), and while reduced food competition associated with population decline may cause increased growth rates (and hence higher chances of precocial breeding), selection may have played a role in the shift to precocial breeding (Lachish et al., 2009). Further, a genome-wide association study has suggested that susceptibility to DFTD may have a genomic basis, indicating that there may be genetic variance required for the population to mount an adaptive response (Margres et al., 2018). Finally, selection by DFTD appears to swamp out selection by local abiotic factors (Fraik et al., 2020), indicating the ecological importance of the disease.

In this study, we applied quantitative genetic analyses to data collected from a closely-monitored wild population of Tasmanian devils on Freycinet Peninsula, on the east coast of Tasmania, to estimate the potential for an evolutionary response following the emergence of DFTD. In particular, we used genomic relatedness data to estimate the extent of genetic variation and/or inbreeding depression in susceptibility to DFTD, as well as to measure the phenotypic and genetic correlations between susceptibility to DFTD and body size. In Tasmanian devils, body size may be subject to disease-induced selection as size commonly predicts social dominance, which in turn increases the frequency of the types of social interaction which result in disease transmission (Hamede et al., 2008, 2009; Hamilton et al., 2020). If we assume susceptibility to DFTD directly correlates with a component of individual fitness (i.e., survival), then the phenotypic and genetic correlations of individuals' DFTD infection status with size traits should approximate the predicted change in size traits resulting from selection induced by DFTD (Price, 1970; Robertson & Lewontin, 1968). Under these general predictions, we specifically aimed to (1) identify phenotypic and genetic correlations between susceptibility to DFTD and size, (2) estimate genetic variation in susceptibility to DFTD, and (3) test for inbreeding depression by estimating the relationship between inbreeding and susceptibility to DFTD or size traits (i.e., head width and body weight).

Materials and Methods

Tasmanian devil study site, trapping and phenotypic data

We used data collected between January 1999 and May 2021 during an ongoing mark-recapture study of Tasmanian devils on the Freycinet Peninsula, Tasmania, Australia. DFTD first

appeared at this site in 2001, resulting in two years' data pre-disease emergence followed by 20 years of data after disease arrival, as the population descended into long-term decline. Tasmanian devils were trapped across the entire 160 km^2 peninsula up to four times a year using custom-built baited traps (Lachish et al., 2007), with trapping periods timed to coincide with key stages in the breeding cycle: autumn (April/May), small pouch young; winter (July/August), large pouch young; spring (October/November), females lactating with young in dens; summer (January/February), dependent young emerging from dens. At their first capture, devils were sexed, individually tagged with an ear tattoo (from 1999 to 2004) or a microchip (after 2004) and a 3mm biopsy sample of tissue taken from the outer edge of the ear for genetic analysis (see below). At first capture and then at all subsequent recaptures their age, head width (in mm) and body weight (in kg) were recorded as described in (Lachish et al., 2007). We use head width as a linear measure of body size because it is precise, as measured across the bony jugal arches of the skull covered by skin with no muscle or fat deposits. Pouch-young of trapped females were sexed and measured, but ear tissue samples were generally not taken because this would result in larger biopsy scars as the individual grew to adult size. A small number of matched pouch-young and mothers were sampled between 2000 and 2003, with 2mm biopsy tissue samples taken from N = 64 pouch young of N = 27 mothers and subsequently sequenced (see below). This allowed us to use these known relatives to assess accuracy and precision of genetic relatedness estimation (see below for details). Individuals were aged using a combination of head width, molar eruption, molar tooth wear and canine over-eruption (Jones, 2023), and given a birthdate of April 1st for a given year, as per Lachish et al. (2007). This method of aging is accurate up to two years of age, but most individuals were first trapped as juveniles and were therefore of precisely known age. Disease status (presence/absence) was determined for each capture by visual inspection for tumours and/or histopathological examination of tumour biopsies (Hamede et al., 2015). The total number of capture records across the 22 years was 2156 across 972 individuals, giving an average number of captures per individual was 2.31 (min = 1, max = 11), and DFTD was confirmed in 10% of these captures with 17% of individuals caught with DFTD at least once. Average age at capture was 22 months (inter-quartile range = 16 – 31 months), and average age at capture with infection was 27 months.

The analyses presented in this study used two different subsets of the full dataset collected during the long-term project. For both datasets, we only included observations from 'adult' individuals at least 14 months old. This was done (1) to minimize conflation of age and size

measurements, and (2) because this is the age at which female devils can be sexually mature such that biting interactions begin and they can thus be at risk of contracting DFTD (Jones et al., 2008). The first dataset was used for analyses of phenotypic relationships (see *Statistical analysis* section below). After removing observations of individuals younger than 14 months and those where there were missing data, this dataset consisted of 1550 recaptures of 729 individuals (hereafter "phenotypic dataset"; 354 males and 375 females). The second subset only included captures of individuals for which we also had genetic data in addition to phenotypic data. Genetic data (described below) were used to estimate genetic relatedness and inbreeding coefficients needed for quantitative genetic analyses to estimate additive genetic variance (V_A) and inbreeding depression, as well as genetic covariances between traits (see *Statistical analysis* section below for details). This latter dataset used for quantitative genetic analyses comprised of 498 observations of 243 individuals (hereafter "genetic dataset"; 121 males and 122 females).

DNA extraction and genotyping

We extracted DNA from tissue samples and conducted genotyping as previously described elsewhere (Epstein et al., 2016; Margres et al., 2018). Briefly, single-nucleotide polymorphism (SNP) genotyping was achieved via single-digest *RADcapture* (i.e., "Rapture" (Ali et al., 2016)) of DNA extracted from tissue. All raw reads from sequencing were first aligned to to the *S. harrisii* reference genome (Murchison et al., 2012). The first round of sequencing that was conducted with this population resulted in data that were of low sequencing depth. As a result, most samples were subsequently re-sequenced in another run to achieve deeper sequencing depth, thereby improving genotyping accuracy. Reads generated from these replicate runs of the same individuals were merged after aligning to the reference genome, and SNP calling was conducted using the merged "bam" files using the stacks pipeline as in (Stahlke et al., 2021). PCR duplicates were removed and SNPs were discovered and called using *gstacks* (Catchen et al., 2013). The function *populations* was then used to filter SNPs to keep one random SNP per RAD locus and per 10Kb window, exclude SNPs with a minor allele frequency (MAF) below 1%, remove individuals with more than 70% missing data, and remove SNPs that were present in less than 50% of the samples. We then further filtered genotype calls with a read depth of less than 4 in order to increase genotyping accuracy, before reapplying the filtering parameters explained above. This resulted in a total of 2105 SNPs genotyped in a total

of 584 individuals for the whole study population (which was further restricted for use in further analyses – see below).

Genomic relatedness estimates

Quantitative genetic analyses used to partition phenotypic variance into additive genetic and environmental effects are often achieved via a pedigree (Kruuk, 2004; Wilson et al., 2010), which can be based on field observations and/or constructed using genetic marker data. Unfortunately, irrespective of the SNP filtering parameters we used, we were unable to determine sufficient numbers of parentage assignments for a pedigree that could be used for analyses: of 651 individuals, we were only able to assign maternities to 160 and paternities to 175 (N = 83 individuals with both parents assigned). We were also only able to match 40 of 64 known mother-offspring (pouch young) relationships, with the remaining 24 either not assigned to a mother or mismatched. We therefore ran our quantitative genetics models using a genomic relatedness matrix (GRM) instead of a pedigree (Bérénos et al., 2014; Gervais et al., 2019). It has been suggested that running these models with a GRM may in fact improve the accuracy of quantitative genetics parameters estimated via these models, especially when pedigree depth is relatively shallow (Gienapp et al., 2017).

To estimate a GRM, we first filtered the set of SNP loci to improve the precision and accuracy of the GRM, following Gervais et al. (2019). SNPs were filtered for a MAF of at least 10% and missingness no greater than 50%, resulting in a set of 1811 SNPs. Prior to calculating the final GRM, we first used the filtered SNP set to identify and remove possible duplicate pairs of individuals contained in the dataset. Duplicate pairs of individuals may occur in cases where, for instance, an individual identification is lost (unreadable tattoo or failure to locate a microchip) on recapture, and they are treated as a new individual and given a new identification. Duplicate individuals were identified and removed from analyses using pairwise relatedness and confirmed via matched life-history data. To do this, we first identified pairs of sequenced samples that had extremely high estimated relatedness (threshold >0.8) and were therefore likely duplicate samples of the same individual. This threshold was selected based on the upper tail of the total distribution of relatedness estimates, assuming that there should be a non-continuous distribution of relatedness values between (truly) highly related pairs and those that are instead duplicates. For each putative duplicated pair, we then cross-referenced with their estimated birth year and sex to ensure that they were indeed duplicates. This procedure

identified 44 pairs of samples, and for each duplicated pair, the sample with the best quality genotyping data was kept. After removing duplicated individuals and re-filtering the SNP dataset according to parameters explained above, the final dataset for estimation of the GRM included 540 individuals and 1808 SNPs. Note that not all of these 540 individuals had phenotypic data for DFTD status associated with them, so therefore not all were included in the statistical analyses below. However, we retained all these individuals for the estimation of the GRM so as to improve precision of allele frequencies of the population required for estimating relatedness.

We next assessed which relatedness estimate performed best at estimating known relatives in this dataset (N = 51 mother – pouch-young pairs in which both individuals had genetic data). Relatedness was estimated using six measures: *Yang* relatedness was estimated using GCTA (Yang et al., 2011), and *Wang*, *Queller and Goodnight*, *Dyad maximum likelihood*, *Lynch*, and *Ritland* estimates were all estimated using COANCESTRY (Wang, 2010). Comparing pairwise relatedness estimates for all mother-offspring pairs (detailed above), the *Wang* relatedness estimate performed best, with an average R value for mother-offspring pairs of 0.47. We therefore used the GRM calculated using *Wang* relatedness estimate in all further quantitative genetic analyses. The variance in pairwise relatedness values using this estimate was 0.007, with approximately 518 pairs of first-degree relatives (i.e., parent-offspring pairs or full siblings, r > 0.45) and 2414 pairs of second-degree relatives (e.g., half-siblings, r = 0.2 – 0.3) (out of a total of 145,530 possible pairs) (Figure S1).

Inbreeding coefficients

We measured variation in inbreeding using genomic inbreeding coefficients estimated in GCTA (Yang et al., 2011). We selected to use $\hat{F}$III (hereafter F_{GRM}), which estimates the allelic correlation between gametes, as this measure has been found to be most closely correlated with runs of homozygosity on the genome (F_{ROH}), and is therefore likely a better measure of the genomic consequences of inbreeding (Yang et al., 2011). We ensured that F_{GRM} measures were robust to SNP filtering by varying the MAF cut-off criterion (1%, 5% and 10%). F_{GRM} estimates were all very highly correlated irrespective of which MAF cut-off we used (r > 0.99%). Our genomic measure of inbreeding, F_{GRM}, ranged from -0.37 (indicating that the individual's parents are not related to each other) to 0.36 (indicating that the individual's parents are highly related to one another) (median F_{GRM} = -0.04, variance = 0.006, Fig S2).

Statistical analyses

In all models, susceptibility to DFTD was fit as a case-control binary variable (1/0 case/control), where "cases" were any capture of a devil with a confirmed DFTD infection, and "controls" were captures of an uninfected individual. Note that we used a dataset containing repeated measures of all individuals, which in some cases means that an individual may first be considered a control before being diagnosed with DFTD at one or more subsequent recaptures. All models were fit in *stan* via the *brms* R package (Bürkner, 2017) using default flat priors on the fixed effects and half-Cauchy priors with 2 degrees of freedom on the random effects. All models were run for 10 000 iterations with a warm-up period of 2000 across four chains, and convergence was assessed by ensuring R-hat was below 1.01, effective sample sizes for all parameters were at least 1000 and by visually ensuring chains had mixed well.

a. Selection on size via DFTD

We estimated the phenotypic relationship between susceptibility to DFTD and size traits by fitting a univariate mixed effects model of the effect of size traits on the probability of having DFTD, using the phenotypic dataset. This model (Model 1; Table 1) fit DFTD occurrence on a given capture with a logit link via the Bernoulli family and included the following fixed effects: *age in months* to account for increased likelihood of contracting the disease as devils age; *sex* to account for any potential sex differences in likelihood of contracting the disease; the interaction between *age* and *sex*; *year* as a covariate to account for the increase in disease presence in the population through time; *head width (mm)* and *body weight (kg)* measured at the same capture. We also fit as multi-level random effects: *year,* to account for repeated measures on multiple years and any non-linear variation between years in disease prevalence; *trap ID*, which described the location of the trap at which individuals were caught (trap locations were consistent across years) and was used to account for spatial environmental heterogeneity across the study area; and *individual ID* to account for repeated measures of individuals.

b. Additive genetic variance (V_A) and inbreeding depression

To test whether there was evidence for variance in additive genetic effects (V_A) or inbreeding depression in any of the phenotypic traits (susceptibility to DFTD, head width, weight), we ran

a suite of univariate animal models using the genetic dataset. Animal models extend linear mixed effects models by incorporating relatedness information to partition phenotypic variance into additive genetic and other sources of variance (Kruuk, 2004; Wilson et al., 2010). We ran a single model for each trait, where DFTD occurrence was fit as a response variable with a logit link via the Bernoulli family (Model 2; Table 1), and head width and body weight were both fit as response variables as Gaussian traits (Model 3 and 4; Table 1).

Animal models were fit with the following fixed effects: *age in months* to account for growth and increased likelihood of contracting disease with age, *year* to account for phenotypic change through time, F_{GRM} to test for evidence for inbreeding depression, and the interaction between *age* and F_{GRM} to test whether the effect of inbreeding changed with age (Marjamäki et al., 2021). Animal models for head width and body weight further included sex, the quadratic effect of age (i.e. age^2), and the interaction between sex and age, and sex and age^2. V_A was estimated in animal models by fitting the genomic relatedness matrix as a covariance matrix. We estimated permanent environment effects variance (V_{PE}) by fitting repeated measures of individuals via a random effect for individual ID. Animal models further included year as a random effect to account for non-linear variation across years (V_{Year}), as well as trap ID (V_{Trap}). Heritability (h^2) for each trait was then estimated as the proportion of phenotypic variance (measured as the sum of all variance components) explained by V_A. We present estimates of heritability for DFTD on both the latent scale and observed data-scale, which was estimated by converting latent-scale variance estimates to the data-scale using the QGGLMM package in R (de Villemereuil et al., 2016). Latent scale heritability can be interpreted as the expected heritability for a hypothetical (latent) trait reflecting overall susceptibility to DFTD, whereas observed data-scale heritability can be interpreted as the heritability of the probability of being diagnosed with DFTD in the population, which incorporates sampling variance in the observed data.

Estimates of V_A can be inflated by maternal effects that are unaccounted for in our models (Kruuk & Hadfield, 2007; Wilson et al., 2005). Unfortunately, in these data, maternities for most individuals were unknown because pedigree reconstruction was not possible with the available SNP dataset (see above for details). However, we explored several alternative methods to quantify maternal effects to examine whether our estimates of V_A were being inflated by maternal effects (see supplement). Estimates of V_A were not substantially inflated by not fitting maternal effects (estimated inflation of h^2 = 1% for DFTD, 5% for weight and

3% for head width, see supplementary Text S1 and Figure S3), and thus we present results without a maternal effects term fit.

Finally, to ensure that the temporal trends in either head width or body weight estimated in their respective models in this section did not arise as an artifact of using the genetic dataset, we ran models with head width and body weight as response variables using the phenotypic dataset that included the same fixed and random effects structure as the animal models (Models 3 and 4; Table 1), but without F_{GRM} or the relatedness matrix.

c. Phenotypic, genetic and other covariances between traits

Phenotypic relationships may be causal if they are associated with a genetic covariance, but may also arise when some component of the environment is affecting each trait in parallel (e.g. (Hajduk et al., 2018)). As such, we next ran analyses to estimate the pairwise genetic covariances between susceptibility to DFTD and each of the two size traits. To do this, we ran a suite of bivariate animal models using the genetic dataset. These models used similar fixed and random effects structures to the univariate animal models explained in section *b*, but were fit without year for head width and weight, and without the interaction between age and F_{GRM} for any trait because these effects were not different from zero and so we chose to remove these terms in order to simplify the models. All were fit with two response traits at a time in order to estimate variance-covariance matrices for each random effect (i.e., V_A, V_{PE}, V_{Year}, V_{Trap}). Specifically, we ran three bivariate models with the following combination of response variables: (1) body weight and head width (Model 5; Table 1); (2) susceptibility to DFTD and head width (Model 6; Table 1); and (3) susceptibility to DFTD and body weight (Model 7; Table 1) (note that a single trivariate model of all three traits had convergence problems). Re-fitting bivariate models with a 'body condition index' (i.e., body weight divided by head width) did not qualitatively change the results presented. As explained above, bivariate models including DFTD as a binary variable were fit with a logit link and therefore these models do not estimate a residual covariance between the binary and Gaussian trait (Bürkner, 2021). Therefore, we also fit bivariate models with 'relative DFTD' fit with Gaussian errors, where relative DFTD was calculated by dividing observed DFTD at each observation by the mean probability of having DFTD. These models have the added advantage of directly estimating the selection differential (i.e. covariance) between susceptibility to DFTD and size (see (Price, 1970; Walsh & Lynch, 2018) for a detailed explanation). Although these models suggest that

there was a negative residual covariance between susceptibility to DFTD and both body weight and head width, the overall qualitative inference of other covariance parameters did not change (Table S3 and S4). We therefore present parameter estimates derived from models where DFTD was fit with a logit link. All models estimated both covariances and correlations for each random effect and we present both parameters for comparison.

Finally, the phenotypic relationships estimated in section *a* were estimated from the phenotypic dataset which contained observations of individuals at least 14 months old for which there were complete phenotypic data (N = 1550 recaptures of N = 729 individuals). However, all quantitative genetic analyses used to estimate genetic variances and covariances were run with the genetic dataset which retained observations of individuals with genetic data (N = 498 observations of N = 243 individuals). Therefore, to ensure any differences in the phenotypic and genetic (or environmental) covariances were not artifacts that arose from the use of different datasets, we re-ran the phenotypic model described in section *a* with the genetic data to facilitate a more direct comparison with the estimated covariances.

Results

Selection on size via DFTD

There was no evidence for sex differences in the probability of having DFTD (Table 2). However, the probability of an individual having DFTD increased over the study period, and also with individual age (Table 2). Devils with relatively larger heads had a greater probability of having DFTD, even after correcting for age (Table 2, Figure 1). Furthermore, devils with relatively lower body weight had a higher probability of having DFTD (Table 2, Figure 1).

Additive genetic variance (V_A) and inbreeding depression in morphology and DFTD

In our animal models using the genetic dataset, we found effects of age and age^2 on both head width and body weight, indicating further growth in individuals older than 14 months old (see Table 3). There was also an effect of sex, reflecting sexual dimorphism in the species whereby adult males are larger than adult females (Table 3; average body weight: Males = 8.45 ± 2.02 kg, Females = 6.80 ± 1.48 kg), and an interaction between age and sex indicating greater rates

of increase with age, even after 14 months. There was no evidence for any change over time in either head width or weight, as indicated by the 95% credible intervals for the linear effects of year overlapping zero (Table 3). Tests of temporal changes in either size trait using the larger phenotypic dataset yielded similar results, as both sets of analyses suggested that neither head width nor body weight was changing through time (see Table S2); these models also showed effectively the same sex and age effects as found in the genetic dataset.

Posterior distributions for estimates of additive genetic variance V_A from the animal models were different from zero for all three traits (Table 3, Figure 2). Heritability was estimated at 0.14 (95% CI = 0.02 – 0.29) for head width, and 0.23 for body weight (95% CI = 0.09 – 0.38). Heritability for susceptibility to DFTD was estimated at 0.40 on the latent scale (95% CI = 0.12 – 0.71) and 0.07 (95% CI = 0.02 – 0.12) on the observed data-scale (Figure 2). All three traits also showed permanent environment effects variance (V_{PE}), but V_{PE} was substantially lower than V_A in susceptibility to DFTD (Figure 2, Table 3). Phenotypic variation associated with spatial heterogeneity (as measured using *Trap ID*) was relatively small but non-zero for all three traits (Table 3 and Figure 2).

There was no evidence for an effect of F_{GRM} on either head width or susceptibility to DFTD: the posterior distribution for the effect of F_{GRM} on both traits centred close to zero (Table 3), suggesting that there was no evidence of inbreeding depression in either head width or susceptibility to DFTD. The 95% CI for the effect of F_{GRM} on body weight also overlapped zero (-3.79 - 0.39), suggesting no statistical support for inbreeding depression in body weight. The posterior distribution did indicate that there was a 94% probability that the relationship between F_{GRM} and body weight was negative, although there remains a 6% probability that the effect of F_{GRM} is either positive or zero (Table 3, Figure 3). In identifying F_{GRM} for genotyped individuals, we found that there were approximately 8 individuals in the dataset that appeared very outbred (i.e., $F_{GRM} < -0.3$). This may arise as an artifact of the dataset (e.g., excess heterozygosity caused by sequencing error), but there was nothing in the data of these individuals that suggested that this was not a biological signal and this level of outbreeding may have emerged, for example, as a result of those individuals being immigrants to the study site. Nonetheless, removing these very outbred individuals did not change our inferences about inbreeding depression in this dataset.

Phenotypic, genetic and other covariances between traits

Head width and body weight: The total phenotypic covariance between head width and body weight, estimated as the sum of all covariances from the bivariate model, was positive (COV_P = 3.40; 95% CI = 2.45 – 4.47). The permanent environment effects covariance between head width and body weight was strongly positive (Table 4). There was no statistical support for a positive genetic covariance between head width and body weight as posterior distributions overlapped zero, although 91% of the posterior distribution was positive. The covariances for both other terms (year and trap) were not different from zero (Table 4).

DFTD and head width: There was no evidence for an overall phenotypic covariance between susceptibility to DFTD and head width, estimated as the sum of all covariances in a bivariate model using the genetic dataset (COV_P = 3.51; 95% CI = -8.34 – 20.97). There was no statistical support for either a genetic or a permanent environment covariance between the traits as the posterior distributions for both were wide and overlapped zero (Table 4, Figure S4). Posterior distributions for both other terms (year and trap) also overlapped zero. The results are in contrast to the positive phenotypic association between susceptibility to DFTD and head width estimated from the phenotypic dataset in section *a*, which may have been because the phenotypic associations between size traits and susceptibility to DFTD were estimated as relative to each other (i.e., body weight relative to head width and vice versa). However, when we re-ran the phenotypic selection model with the genetic dataset, we again found no phenotypic association between susceptibility to DFTD and head width (see Table S1), suggesting instead that the contrasting conclusions concerning the strength of statistical support for the association between DFTD and head width likely occurred from differences between the two datasets.

DFTD and body weight: When fitting susceptibility to DFTD as a binary variable, we found that the total phenotypic covariance between susceptibility to DFTD and body weight, estimated as the sum of all covariances in a bivariate model, was clearly negative (COV_P = -2.69; 95% CI = -7.77 – -0.71). The overall negative association was also confirmed when we re-ran the phenotypic selection model with the genetic dataset, where we found a negative phenotypic association between susceptibility to DFTD and body weight (see Table S1). We found a negative genetic covariance between the two traits, estimated at -2.56 (posterior median; 95% CI: -6.11 - -0.50). However, posterior distributions for the permanent

environmental effects covariance between susceptibility to DFTD and body weight, as well as the covariances for the year and trap terms, were wide and overlapped zero (Table 4, Figure S4). Although the credible interval for the genetic covariance was different from zero, posterior distributions for covariance estimates were all quite wide and uncertain.

Discussion

Our analyses of a long-term dataset of Tasmanian devils revealed evidence of additive genetic variance in susceptibility to DFTD, suggesting that there is adaptive potential for Tasmanian devils to evolve resistance to DFTD. There was no statistical evidence for inbreeding depression in susceptibility to DFTD, head width, or body weight. Finally, whilst there was evidence for a positive phenotypic relationship between head width and susceptibility to DFTD, this was not associated with a genetic covariance, whereas there was evidence that the negative phenotypic relationship between weight and susceptibility to DFTD was underpinned by a negative genetic covariance.

Additive genetic variance in a trait will determine the evolutionary response to selection on that trait (Golas et al., 2021; Walsh & Lynch, 2018). Our estimates of V_A indicate a genetic basis to susceptibility to DFTD in Tasmanian devils, which may result in the population evolving resistance to the disease. This result aligns with those from a genome-wide association study which suggested that major effect loci explain a significant proportion of variation in the probability of having DFTD (Margres et al., 2018), and is also consistent with several previous studies indicating rapid evolutionary responses of devils as evidenced by allele frequency changes at some loci across the genome (Epstein et al., 2016; Fraik et al., 2020; Stahlke et al., 2021). Together with these previous studies, our results suggest there may be some potential for the population to respond adaptively to DFTD. Strong directional selection on any fitness-related trait should eventually deplete additive genetic variance as alleles at causal loci move towards fixation (Bulmer, 1971). We may therefore expect that additive genetic variance in susceptibility to DFTD should decrease over time as the population evolves resistance. Alternatively, additive genetic variance may be maintained as a result of the continued evolution of DFTD, resulting in arms-race style host-pathogen coevolution (Best et al., 2008; Boots et al., 2009; Stammnitz et al., 2023). The realised evolutionary response in this population will therefore be the product of selection acting on both devils and DFTD, as well as the ecological environment in which devils live and are exposed to the disease. Additionally, while our analyses focused on the resistance to DFTD, it is highly likely that tolerance to DFTD

is also evolving in the population (Hamede et al., 2020). In situations such as this, tolerance could be assessed from an individual's survival following infection. However accurately measuring disease tolerance in mark-recapture studies can be inhibited by recapture probabilities, and future work could focus on incorporating data on survival post infection to investigate how disease tolerance evolves in populations facing EIDs.

Inbreeding depression occurs when recessive deleterious mutations are expressed as homozygotes as a result of inbreeding and negatively impact traits associated with fitness in a population (Charlesworth & Willis, 2009; DeRose & Roff, 1999). Interestingly, despite DFTD being a reliable predictor of survival, we did not find evidence for inbreeding depression in susceptibility to DFTD. Furthermore, whilst body weight is often directly related to fitness via condition-related survival and reproduction, and has been found to be subject to inbreeding depression in many wild animals (Hajduk et al., 2018; Huisman et al., 2016; Laikre & Ryman, 1991; Nielsen et al., 2012), we did not find statistical support for inbreeding depression in body weight. Inbreeding depression in Tasmanian devils would be especially concerning considering the repeated historical population bottlenecks and recent steep declines in population size (Brüniche-Olsen et al., 2013, 2014; Lachish et al., 2007; Patton et al., 2020), and so the overall lack of evidence for inbreeding depression is positive when assessing the probability of the population's persistence. This is an interesting finding given that inbreeding depression has been found in other Tasmanian devil populations (R. M. Gooley et al., 2020), although studies of captive Tasmanian devils have also found a lack of inbreeding depression (R. Gooley et al., 2017). One explanation for the overall lack of inbreeding depression could be that recessive, deleterious alleles have already been purged from the population (Grossen et al., 2020; Hedrick & Garcia-Dorado, 2016; Kirkpatrick & Jarne, 2000) either via inbreeding or during the repeated population bottlenecks experienced across the species' range. Nonetheless, the expression of inbreeding depression may be dependent on both environmental conditions and genetic diversity within the population (Hedrick & Kalinowski, 2000), and whilst a lack of inbreeding depression provides a positive outlook for the population now, it does not protect against inbreeding depression in the future.

Phenotypic and genetic covariances between DFTD and size traits can be used to predict whether either size trait will respond to selection caused by the disease (Price, 1970; Robertson & Lewontin, 1968), on the assumption that DFTD is a strong predictor of survival and hence fitness. We found that weight and susceptibility to DFTD were phenotypically and genetically

518 negatively correlated. It is important to note that our phenotypic analyses tested the effect of
519 head width and body weight on DFTD concurrently and therefore our results reflect the effect
520 of relative measures of each size trait. This means that we found that individuals with *relatively*
521 greater body weight for a given head width (i.e. skeletal size) were less likely to have DFTD.
522 The phenotypic covariance between these traits may reflect an immunocompetence - body-
523 condition relationship, whereby (relatively) heavier individuals are in better condition and
524 consequentially have better resistance to disease (Gleeson et al., 2005). Alternatively, the
525 directionality of causality in the phenotypic covariance may be reversed whereby individuals
526 that have the disease subsequently lose weight (Sánchez et al., 2018). As the observed negative
527 phenotypic covariance was mirrored by a negative genetic covariance, this suggests that the
528 relationship is more likely an indirect measure of body-condition positively impacting immune
529 function (Gleeson et al., 2005).

530 We found that there was a positive phenotypic covariance between head width and
531 susceptibility to DFTD at the phenotypic level, but we did not find evidence for this being
532 underpinned by a genetic covariance. The underlying mechanisms causing the phenotypic
533 relationship between susceptibility to DFTD and head width remain unclear, although one
534 possibility is that the association may reflect an indirect association with social dominance. For
535 instance, assuming that head width accurately predicts social dominance and males' access to
536 mates in the breeding season when much of the transmission-relevant injurious biting occurs,
537 the relationship between head width and susceptibility to DFTD may reflect a greater
538 probability of infection caused by increased rates of the interactions that cause disease
539 transmission that occur in socially dominant individuals (Hamede et al., 2008, 2009; Hamilton
540 et al., 2019). Interestingly, we found that this relationship was not associated with a genetic
541 covariance. However, re-running the phenotypic model with a smaller dataset did not indicate
542 the same phenotypic relationship between susceptibility to DFTD and head width, suggesting
543 that it is more likely that this dataset was limited in its statistical power to detect the phenotypic
544 relationship, and therefore presumably also any associated genetic or environmental
545 covariances.

546 In conclusion, EIDs are thought to dramatically alter the evolutionary dynamics of wild
547 populations (Rogalski et al., 2017), but empirical evidence of this process is rare. We show that
548 in an endangered marsupial facing an EID that has had a catastrophic impact on the species,
549 there is evolutionary potential in disease traits and current and ongoing selection acting on

correlated morphological traits. Critically, we show that susceptibility to DFTD and size traits are all associated with underlying heritable genetic variance. We also show that these patterns exist in the absence of inbreeding depression. These results therefore not only provide important empirical evidence for how EIDs may shape future evolutionary dynamics of a population, but critically suggest that the species may hold the adaptive potential required to avoid extinction.

Acknowledgements

We would like to first acknowledge the Toorerno-maire-mener clan, the Traditional Custodians and First Peoples of the Freycinet Peninsula where this project was delivered, and we pay respect to their Elders past, present and emerging. We would also like to thank the many researchers involved in field sampling during the course of the study. We also thank Soraia Barbosa for facilitating the sharing of the genetic data. KS is funded by a European Research Council grant to LEBK; LEBK is funded by the Royal Society of London; genetic sequencing data was funded by the following grants awarded to AS and PH: NSF DEB-2027446, NIH R01-GM12653, NSF Ecology of Infectious Diseases Award #DEB-1316549; the long-term mark recapture field study was supported by the following grants: Australian Research Council Discovery DP110102656, Australian Research Council Linkage Grant - LP0989613, Australian Research Council Linkage Grant - LP0561120, Australian Research Council Large Grant - A00000162, Australian Research Council Future Fellowship FT100100031 to MJ, Australian Research Council Australian Postdoctoral Fellowship to MJ.

Figure 1. Plot showing the relationship between head width and DFTD (a), and weight with DFTD (b). Points show observed data, and regression lines show the predicted relationship between size traits and DFTD derived from a mixed effects model which fits DFTD as a case-control response as a function of both size traits (see methods for full model structure). Solid dark line shows predictions derived from the median of the posterior and the lighter lines show 100 randomly selected draws from the posterior distribution.

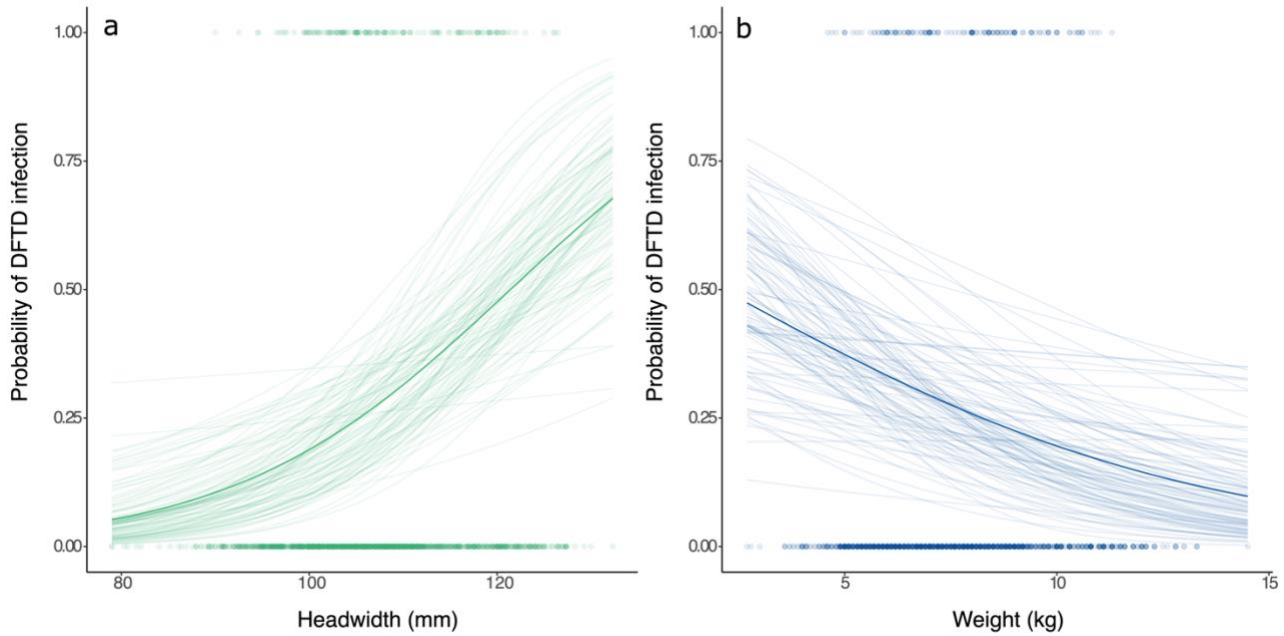

Figure 2. Plot showing proportion of phenotypic variance in DFTD, head width and weight attributed to variance in additive genetic effects (V_A) (reflecting narrow-sense heritability (h^2)); permanent environment effects (V_{PE}); year (V_{Year}) and spatial location (V_{Trap}). Variances for DFTD shown on the observed data-scale (see Table 2 for estimates on latent-scale). Posterior median of estimates shown as point, with 75% CI's shown as heavy lines and 95% CI's as lighter line.

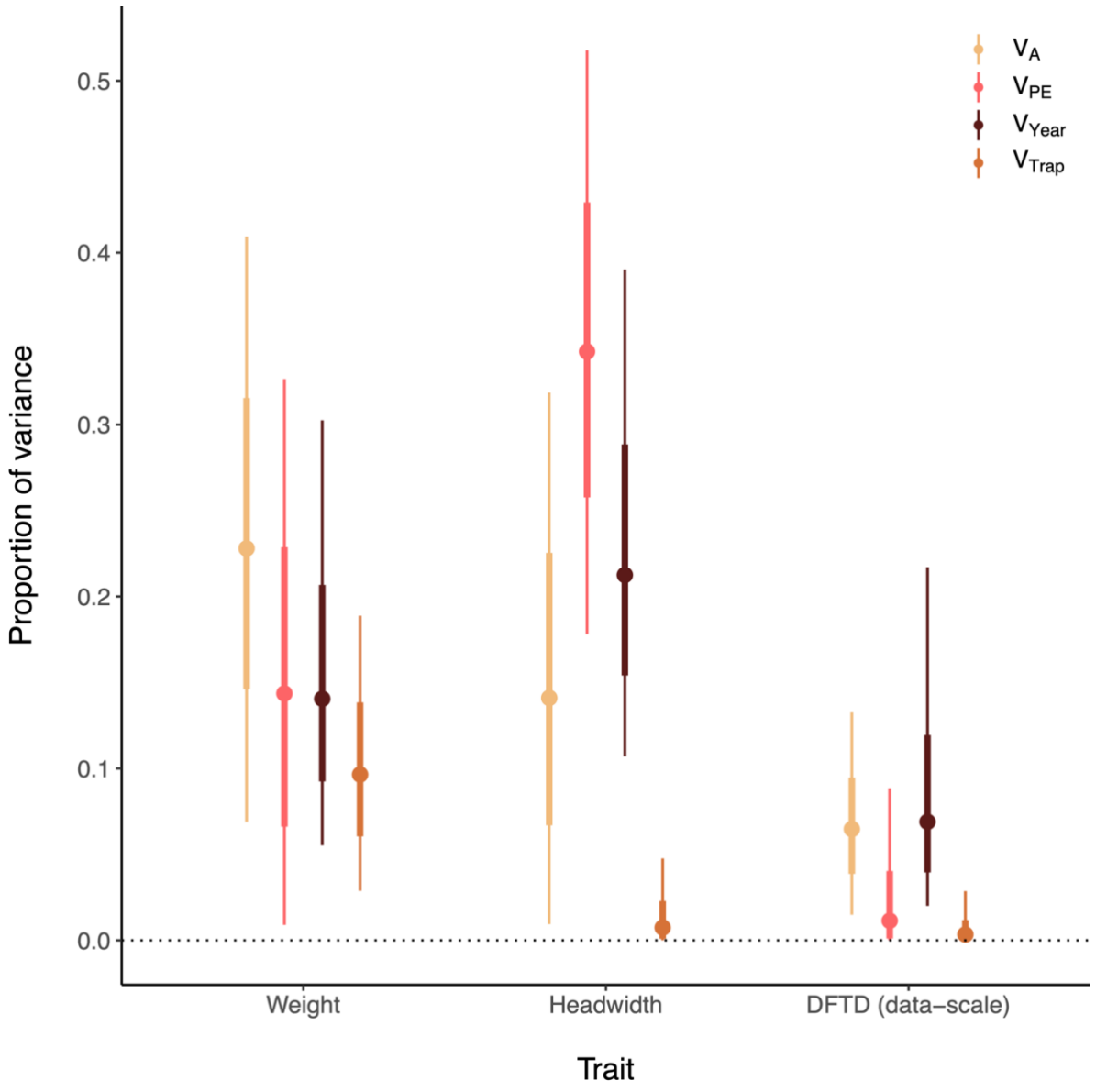

Figure 3. Plot showing relationship between F_{GRM} (i.e., $\hat{F}$III) and body weight. Points show raw, observed data, and regression lines show the predicted relationship between F_{GRM} and body weight, where the solid dark line shows predictions derived from the median of the posterior and the lighter lines show 100 randomly selected draws from the posterior distribution.

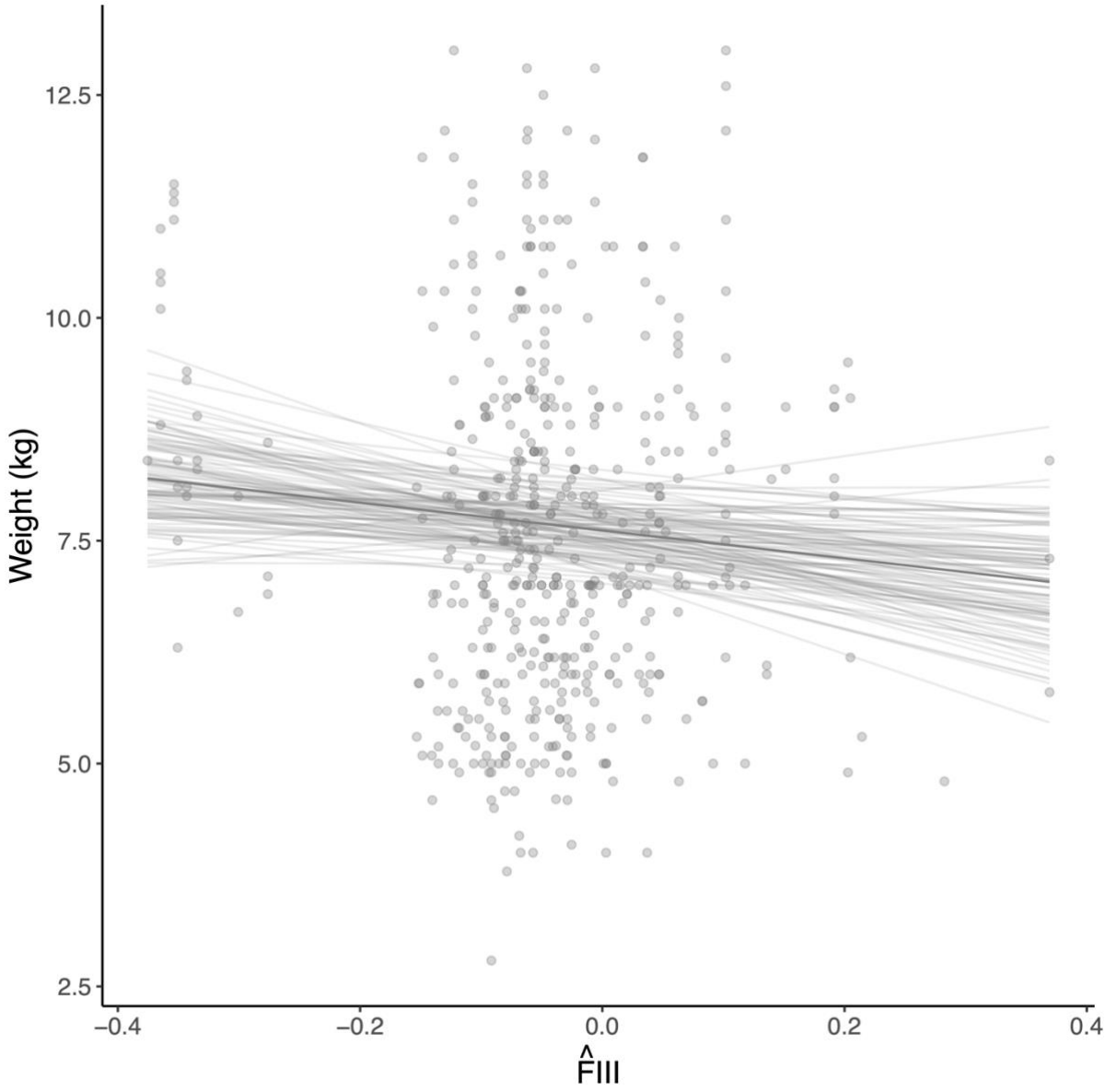

Table 1. Table outlining the structure of all linear mixed effects models outlined in *statistical analyses* section. All models were fit in stan via the brms package in R. *Model* refers to the model number referenced in text; *Response* refers to the response variable fit in the model; *Fixed effects* describes the fixed effects structure used in the model, where a colon represents an interaction term between two fixed effects; *Random effects* describes the random effects structure; *Family (link function)* describes the family with which the response variable was fit. Note that in bivariate models, the fixed effects structures varied between response variables and are shown on separate rows.

Model	Response	Fixed effects	Random effects	Family (link function)
	Univariate			
1	DFTD	Age + Sex + Year + Head width + Body weight	Year + Trap + ID	Bernoulli (logit)
2	DFTD	Age + Year + F_{GRM} + Age:F_{GRM}	Year + Trap + ID + *a*	Bernoulli (logit)
3	Head width	Age + Age^2 + Sex + Year + F_{GRM} + Age:F_{GRM} + Age:Sex + Age^2:Sex	Year + Trap + ID + *a*	Gaussian
4	Body weight	Age + Age^2 + Sex + Year + F_{GRM} + Age:F_{GRM} + Age:Sex + Age^2:Sex	Year + Trap + ID + *a*	Gaussian
	Bivariate			
5	Head width ; Body weight	Age + Age^2 + Sex + Age:Sex + Age^2:Sex + F_{GRM} ; Age + Age^2 + Sex + Age:Sex + Age^2:Sex + F_{GRM}	Year + Trap + ID + *a*	Gaussian Gaussian
6	Head width ; DFTD	Age + F_{GRM} + Year + Age^2 + Sex + Age:Sex + Age^2:Sex ; Age + F_{GRM} + Year	Year + Trap + ID + *a*	Gaussian Bernoulli (logit)
7	Body weight ; DFTD	Age + F_{GRM} + Year + Age^2 + Sex + Age:Sex + Age^2:Sex ; Age + F_{GRM} + Year	Year + Trap + ID + *a*	Gaussian Bernoulli (logit)

Age: linear covariate describing age of individual in months; *Sex*: two-level effect "Male" or "Female"; *Year*: year of observation: *Head width:* in mm; *Body weight*: in kg; $F_{GRM:}$ individuals inbreeding coefficient; Age^2: the quadratic of age in months: *Trap:* the name of the location the observation was taken; *ID*: individual microchip; *a*: additive genetic variance, estimated by fitting genomic relatedness matrix as a covariance matrix.

Table 2. Table summarising results from a mixed effects model used to estimate phenotypic relationship between size traits (body weight and head width) and DFTD occurrence. Response variable is the occurrence of DFTD at a given capture of an individual, fitted as a binary trait. *TrapID* fitted the location of the trap where the individual was caught. Posterior medians of linear coefficient estimate for fixed effects and variance estimates for random effects are presented with 95% credible intervals of posterior distribution in parentheses. Fixed effect estimates where the 95% CI's do not overlap with zero are given in bold. Parameter estimates are on the logit link scale. The dataset used is the phenotypic data set with N = 729 individuals over N = 1550 captures, 22 years and 185 traps.

Parameter		
Fixed Effects	Sex_M	-1.30 (-4.39 - 1.14)
	Head width (mm)	**0.32 (0.11 - 0.75)**
	Body Weight (kg)	**-0.83 (-2.18 - -0.09)**
	Age (months)	**0.29 (0.10 - 0.83)**
	Year (continuous variable)	**1.16 (0.48 - 3.02)**
Random effects variance components	ID	7.31 (3.08 - 19.20)
	Year	4.87 (1.89 - 12.85)
	TrapID	1.87 (0.12 - 5.84)

Table 3. The results of animal models estimating V_A and the effect of F_{GRM} on three traits: head width, body weight and probability of having DFTD (DFTD). Posterior medians of all effects are presented with 95% credible intervals of posterior distributions in parentheses. Fixed effect estimates where the 95% credible intervals of the posterior does not overlap with zero are in bold. Variance components and proportion of phenotypic variance for susceptibility to DFTD are shown on the latent (logit link) scale (estimates on the data-scale can be found in Figure 2). Estimates where posterior distribution does not overlap with zero in bold. The dataset used has N = 243 individuals over N = 498 captures and 19 years and 128 traps.

		Head width	Body Weight	DFTD
Fixed Effects	Age	**1.19 (0.96 - 1.42)**	**0.22 (0.16 - 0.28)**	0.35 (0.12 - 0.75)
	Age^2	**-0.01 (-0.02 - -0.01)**	**-0.002 (-0.003 - -0.001)**	-
	Sex_M	-3.57 (-7.34 - 0.24)	-0.53 (-1.15 - 0.45)	-
	F_{GRM}	-1.97 (-8.62 - 4.90)	-1.68 (-3.79 - 0.39)	-0.88 (-8.33 - 6.76)
	Year	-0.17 (-0.43 - 0.09)	-0.01 (-0.06 - 0.04)	1.68 (0.63 - 3.49)
	$Age:Sex_M$	**0.57 (0.31 - 0.84)**	**0.12 (0.05 - 0.19)**	-
	$Age^2:Sex_M$	**-0.01 (-0.02 - -0.01)**	**-0.002 (-0.003 - -0.002)**	-
Random effects variance components	V_A	4.74 (0.76 - 10.11)	0.36 (0.14 - 0.61)	34.83 (6.17 - 220.55)
	V_{PE}	11.53 (6.92 - 16.96)	0.22 (0.03 - 0.45)	5.91 (0.05 - 60.41)
	V_{Year}	7.08 (3.66 - 14.34)	0.21 (0.09 - 0.47)	39.03 (8.23 - 244.43)
	V_{Trap}	0.25 (0.002 - 1.30)	0.15 (0.06 - 0.27)	1.89 (0.02 - 19.63)
	V_R	9.25 (7.89 - 10.93)	0.56 (0.47 - 0.66)	-
Proportion of phenotypic variance	h^2	0.14 (0.02 - 0.29)	0.23 (0.09 - 0.38)	0.40 (0.12 - 0.71)
	ICC^{PE}	0.34 (0.20 - 0.49)	0.15 (0.02 - 0.30)	0.07 (0.001 - 0.38)
	ICC^{Year}	0.21 (0.12 - 0.36)	0.14 (0.07 - 0.27)	0.44 (0.19 - 0.72)
	ICC^{Trap}	0.007 (0.0001 - 0.04)	0.38 (0.24 - 0.52)	0.02 (0.0002 - 0.13)

Linear coefficient estimates shown for fixed effects. Variance estimates shown for all random effects: variance in additive genetic effects (V_A); permanent environment effects (V_{PE}); year (V_{Year}); spatial location (V_{Trap}) and residual (V_R). Proportion of total phenotypic variance (i.e., sum of all variance components) attributed to additive genetic effects, also known as narrow-sense heritability (h^2); permanent environment effects (intraclass correlation, ICC_{PE}); year (ICC_{Year}); and spatial location (ICC_{Trap}).

Table 3. The results of the three bivariate models used to estimate covariances between head width, body weight and DFTD. Models were fit with DFTD as a binary variable with a logit link. Posterior medians of all covariance estimates presented with 95% credible intervals of posterior distribution in subscript parentheses. Covariances with DFTD given on the latent scale. Full variance-covariance matrices from models can be found in supplementary material (Table S4). Covariance estimates where posterior distribution does not overlap with zero in bold. The dataset used has N = 243 individuals over N = 498 captures and 19 years and 128 traps.

	Head width and Body Weight	DFTD and Head width	DFTD and Body Weight
COV_A	0.94 (-0.02 - 2.49)	-2.63 (-13.34 - 5.91)	**-2.56 (-6.11 - -0.50)**
COV_{PE}	**2.03 (0.87 - 3.14)**	0.26 (-5.40 - 6.18)	0.05 (-0.84 - 0.93)
COV_{Year}	-0.31 (-0.99 - 0.33)	6.78 (-2.18 - 21.16)	-1.06 (-3.43 - 0.53)
COV_{Trap}	0.02 (-0.08 - 0.17)	0.23 (-0.42 - 1.37)	0.29 (-0.12 - 1.02)
COV_{Res}	**0.74 (0.47 - 1.04)**	-	-
COV_P	**3.40 (2.45 - 4.47)**	3.51 (-8.34 - 20.97)	**-2.69 (-7.77 - -0.71)**

Covariance estimates for additive genetic effects (COV_A), permanent environment effects (COV_{PE}), year effects (COV_{Year}), location effects (COV_{Trap}) and residual effects (COV_{Res}). Total phenotypic covariance between each pair of traits (COV_P) given as the sum of all covariances estimated from bivariate models.

660 **Supplementary materials**

661

662 **Figure S1**. Distribution of pairwise relatedness values used in all quantitative genetics models

663 (see main text). Relatedness values estimated using Wang relatedness estimate in COANCESTRY

664 (Wang, 2010).

665

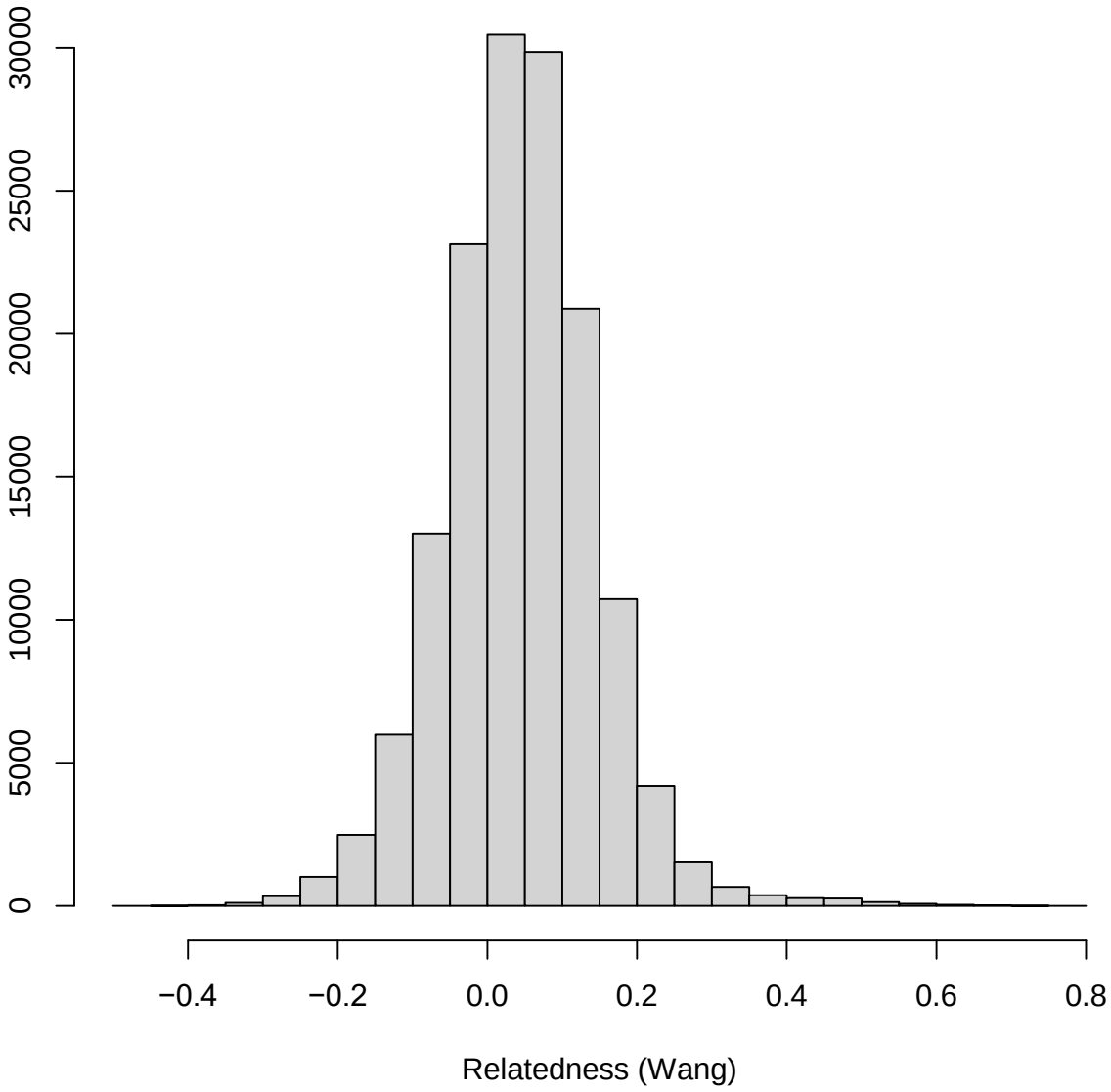

666
667
668
669
670
671

Figure S2. Distribution of individual inbreeding coefficients as estimated by F_{GRM} values. F_{GRM} was estimated using $\hat{F}_{III}$ in GCTA (Yang et al., 2011), which approximates relatedness between an individual's parents, averaged across all loci. More inbred individuals have higher values and more outbred individuals have negative values.

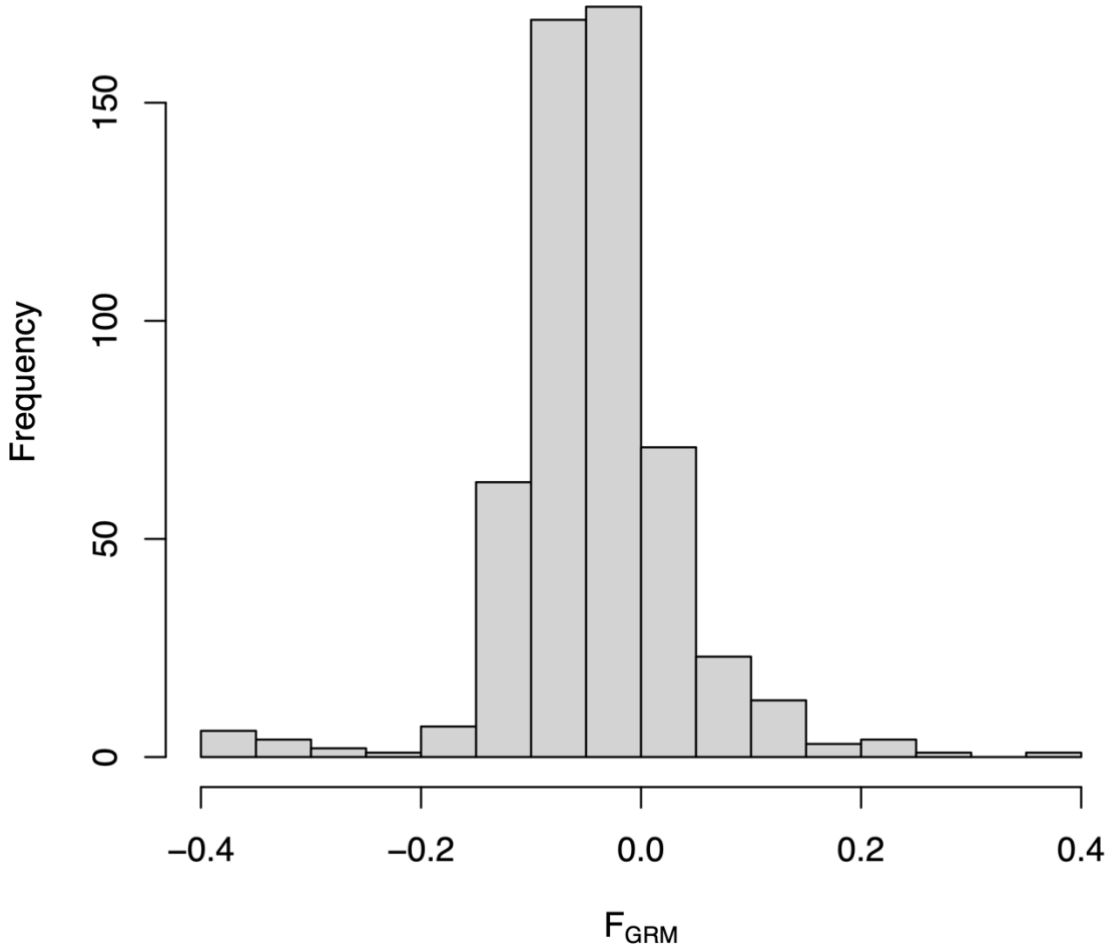

687 **Table S1.** Results from phenotypic model run with the smaller subset of data as used in the
688 quantitative genetic analyses, containing only individuals that had sufficient quality genetic
689 data. *TrapID* is the location of the trap where the individual was caught. The values shown are
690 the posterior medians of linear coefficient estimates for fixed effects and of variance estimates
691 for random effects, with 95% credible intervals of posterior distributions in parentheses.
692 Estimates where the 95% CI does not overlap zero are shown in bold.
693
694

Parameter		
Fixed Effects	SexM	-0.45 (-6.70 - 5.82)
	Head width	0.26 (-0.49 - 1.12)
	Body weight	**-1.55 (-5.58 - 1.40)**
	Age (months)	**0.61 (0.11 - 1.94)**
	Year	**2.14 (0.50 - 5.88)**
Random effects variance components	ID	13.16 (3.69 - 37.71)
	Year	12.88 (3.11 - 40.60)
	TrapID	3.97 (0.22 - 12.37)

695
696
697

698 **Table S2** Results of phenotypic models of head width and body weight used to investigate the
699 temporal trends in each trait. *TrapID* is the location of the trap where the individual was
700 caught. The values shown are the posterior medians of linear coefficient estimates for fixed
701 effects and of variance estimates for random effects, with 95% credible intervals of posterior
702 distributions in parentheses. Estimates where the 95% CI does not overlap zero are shown in
703 bold.
704

		Head width	Body weight
Fixed Effects	Age	0.96 (0.86 - 1.06)	0.20 (0.18 - 0.22)
	Age^2	-0.01 (-0.01 - -0.01)	-0.002 (-0.002 - -0.001)
	Sex_M	-2.21 (-4.39 - -0.04)	-0.15 (-0.59 - 0.30)
	Year	-0.10 (-0.25 - 0.05)	0.004 (-0.02 - 0.03)
	$Age:Sex_M$	0.64 (0.49 - 0.79)	0.12 (0.09 - 0.15)
	$Age^2:Sex_M$	-0.01 (-0.01 - -0.001)	-0.001 (-0.002 - -0.001)
Random effects variance components	ID	3.82 (3.51 - 4.15)	0.82 (0.75 - 0.90)
	Year	2.22 (1.53 - 3.18)	0.45 (0.30 - 0.64)
	TrapID	1.26 (0.83 - 1.70)	0.24 (0.13 - 0.35)

Text S1. <u>Estimating maternal effects without a pedigree.</u>

Estimates of V_A may be inflated if the trait is affected by maternal effects that are not explicitly modelled (Kruuk & Hadfield, 2007; Wilson et al., 2005). Usually, maternal effects are estimated by fitting a vector of known maternities for all individuals in the dataset as a random effect in the model, where maternities have been either observed in the field or identified via a genetically reconstructed pedigree. This option was not possible in our analyses because in our dataset maternities for most individuals were unknown because (1) it is not possible to sample dependent young while with their mother (see main text for details), and (2) pedigree reconstruction was not possible with the available SNP dataset. Nevertheless, we attempted to examine whether estimates of V_A in DFTD or size traits may be being inflated by maternal effects that we were unable to model by using the following two alternative methods.

The first of these methods (*Ped+*) involved re-running our univariate animal models (described in main text) with estimated maternities for all individuals included as an additional random effect. We estimated maternities for all individuals using a combination of maternities from the incomplete pedigree, relatedness estimates and life history information. First, we assigned maternities to individuals if they had been successfully identified during pedigree reconstruction (via the *sequoia* R package (Huisman, 2017). Then, we identified further putative maternities using a combination of relatedness estimates, sex and age. Specifically, we assigned pairs of individuals that putatively may be a mother-offspring pair if they had a relatedness value of more than 0.45, and one of the individuals was a female and was at least 1 year older than the other. That female was then assigned as the possible mother of the other individual. This resulted in a total of 116 putative mothers of 243 individuals contained in the dataset. For the remaining individuals that we did not have a mother estimated, we gave them a unique "dummy" mother.

The second of these methods (*ME Multi R*) was originally proposed by (Zaitlen et al., 2013), and has since been tested and applied in Soay Sheep (James, C et al., 2023). In this approach, maternal effects were estimated by fitting an additional matrix to our univariate animal models which was a modified version of the full GRM that aimed to group individuals that

likely had a shared maternal environment. To create this additional matrix, we truncated the full GRM at a cut-off value such that everything below that value became zero. We did this using two cut-off values of 0.5 (*ME Multi R 0.5*) and 0.25 (*ME Multi R 0.25*). A relatedness of 0.5 was used because this is the expected level of relatedness for both mother-offspring pairs and full-siblings, both of which would have a common maternal environment. We then repeated this with a relatedness of 0.25 in order to also capture maternal half-siblings in this matrix.

We acknowledge that the methods we present here may be imprecise in their estimation of shared maternal environments: the first method may be missing some maternities, whereas the matrices used in the second method retain other types of relatives that do not share a maternal environment. However, we believe that, in combination, these methods are likely effective in assessing the extent that estimates of V_A may be being affected by maternal effects.

We found that for all three traits (body weight, head width and DFTD) fitting a maternal effect using either of the methods we tested reduced estimates of both V_A and V_{PE}. However, the magnitude of difference in our estimates of V_A was very dependent on both the trait and the method we used (Fig S3). Furthermore, the estimates of maternal effects variance were not consistent between the different methods used (Fig S3) and, in all cases, fitting a maternal effect reduced confidence in variance parameter estimates by generating wider posterior distributions. For DFTD, h^2 was estimated around 0.01 higher (on the data-scale) in a model without a maternal effect fitted than when a maternal effect was fit (averaged between the point estimates from the three different methods). For body weight, h^2 was estimated around 0.05 higher in a model without a maternal effect fitted than when a maternal effect was fit (averaged between the point estimates from the three different methods). For head width, h^2 was estimated around 0.03 higher in a model without a maternal effect fitted than when a maternal effect was fit (averaged between the point estimates from the three different methods).

Figure S3. Plot showing proportion of phenotypic variance in DFTD, head width and body weight attributed to variance in additive genetic effects (V_A) (reflecting narrow-sense heritability (h^2)); permanent environment effects (V_{PE}); year (V_{Year}) and spatial location (V_{Trap}) and maternal effects (V_{ME}). Variances for DFTD shown on the observed data-scale (see Table 2 for estimates on latent-scale). Posterior median of estimates shown as point, with 75% CI's shown as heavy linen and 95% CI's as lighter line. V_{ME} estimated using either approximated maternities (*Ped +),* or by fitting an additional matrix which truncated the GRM at a cut-off value (*ME Multi R,* see text S1 for details).

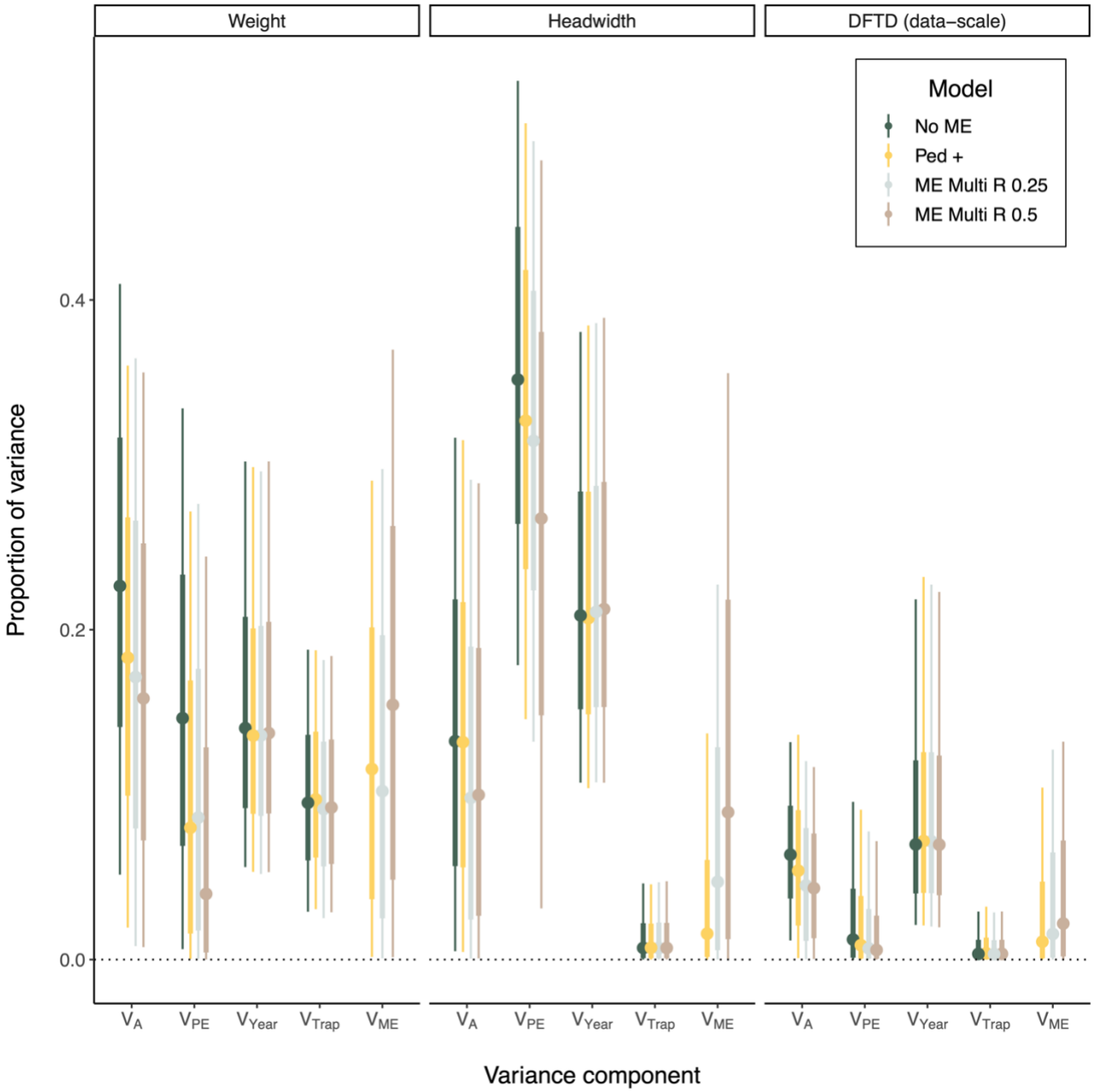

Table S3. The results of the bivariate models used to estimate covariances between head width, body weight and DFTD where models were fit with relative measures of DFTD, body weight and head width (see Methods for details) and were all fit with Gaussian errors. Posterior medians of all covariance estimates presented with 95% credible intervals of posterior distribution in subscript parentheses. Full variance-covariance matrices from models can be found in Table S4.

	DFTD and Head width	DFTD and Body Weight
COV_A	-0.10 (-0.35 - 0.13)	-0.27 (-0.29 - -0.05)
COV_{PE}	0.07 (-0.08 - 0.26)	0.06 (-0.08 - 0.20)
COV_{Year}	0.10 (-0.37 - 0.61)	-0.29 (-0.78 - 0.06)
COV_{Trap}	0.02 (-0.01 - 0.07)	0.04 (-0.01 - 0.12)
COV_{Res}	-0.13 (-0.23 - -0.04)	-0.11 (-0.21 - -0.001)
COV_P	-0.03 (0.55 - 0.50)	-0.57 (-1.09 - -0.26)

Covariance estimates for additive genetic effects (COV_A), permanent environment effects (COV_{PE}), year effects (COV_{Year}), location effects (COV_{Trap}) and residual effects (COV_{Res}). Total phenotypic covariance between each pair of traits (COV_P) given as the sum of all covariances estimated from bivariate models.

Table S4. Full variance-covariance matrices estimated from the three bivariate models used to estimate genetic covariances between DFTD, head width and body weight. Results from each bivariate model shown in turn. For each 2x2 matrix, variances are shown on the diagonal (and shaded in light grey), covariances below the diagonal and correlations above the diagonal. Each estimate is the median of the posterior distribution followed by the 95% CI in parentheses.

		Body Weight	**Head width**
Year	**Body Weight**	0.24 (0.10 - 0.47)	-0.24 (-0.66 - 0.23)
	Head width	-0.30 (-0.99 - 0.33)	8.20 (3.86 - 15.03)
Additive genetic	**Body Weight**	0.28 (0.03 - 0.62)	0.64 (-0.29 - 0.96)
	Head width	0.94 (-0.02 - 2.48)	5.29 (0.10 - 13.35)
Permanent environment	**Body Weight**	0.41 (0.15 - 0.66)	0.93 (0.82 - 0.99)
	Head width	2.03 (0.87 - 3.14)	11.71 (5.47 - 17.59)
Trap	**Body Weight**	0.07 (0.009 - 0.14)	0.05 (-0.84 - 0.84)
	Head width	0.02 (-0.07 - 0.17)	0.34 (0.002 - 1.17)
		Head width	**DFTD**
Year	**Head width**	7.88 (3.65 - 14.45)	0.36 (-0.14 - 0.77)
	DFTD	6.78 (-2.18 - 21.16)	73.94 (6.39 - 212.14)
Additive genetic	**Head width**	5.85 (0.18 - 13.26)	-0.16 (-0.77 - 0.51)
	DFTD	-2.63 (-13.34 - 5.91)	78.39 (5.48 - 274.08)
Permanent environment	**Head width**	11.50 (5.84 - 17.71)	0.04 (-0.82 - 0.87)
	DFTD	0.26 (-5.40 - 6.18)	8.75 (0.02 - 34.69)
Trap	**Head width**	0.38 (0.002 - 1.26)	0.19 (-0.81 - 0.94)
	DFTD	0.23 (-0.42 (1.37)	3.87 (0.01 - 14.73)
		Body Weight	**DFTD**
Year	**Body Weight**	0.28 (0.09 - 0.45)	-0.37 (-0.83 - 0.22)
	DFTD	-1.06 (-3.43 - 0.53)	52.34 (5.64 - 173.06)
Additive genetic	**Body Weight**	0.38 (0.13 - 0.68)	-0.61 (-0.95 - -0.19)
	DFTD	-2.56 (-6.11 - -0.50)	75.40 (7.01 - 256.83)
Permanent environment	**Body Weight**	0.26 (0.05 - 0.48)	0.07 (-0.85 - 0.89)
	DFTD	0.05 (-0.84 - 0.93)	6.46 (0.02 - 26.36)
Trap	**Body Weight**	0.14 (0.05 - 0.25)	0.43 (-0.47 - 0.96)
	DFTD	0.29 (-0.12 - 1.02)	4.73 (0.02-17.76)
		Relative Head width	**Relative DFTD**
Year	**Relative Head width**	0.11 (0.05 - 0.22)	0.11 (-0.34 - 0.56)
	Relative DFTD	0.10 (-0.37 - 0.61)	8.98 (4.24 - 16.43)
Additive genetic	**Relative Head width**	0.08 (0.01 - 0.17)	-0.22 (-0.78 - 0.32)
	Relative DFTD	-0.09 (-0.34 - 0.13)	3.13 (1.47 - 4.96)

Permanent environment	**Relative Head width**	0.14 (0.07 - 0.21)	0.27 (-0.50 - 0.89)
	Relative DFTD	0.07 (-0.08 - 0.26)	0.72 (0.01 - 2.01)
Trap	**Relative Head width**	0.01 (0.0001 - 0.02)	0.41 (-0.57 - 0.96)
	Relative DFTD	0.02 (-0.01 - 0.07)	0.33 (0.01 - 0.84)
Residual	**Relative Head width**	0.12 (0.10 - 0.14)	-0.16 (-0.27 - -0.04)
	Relative DFTD	-0.13 (-0.22 - -0.04)	5.28 (4.44 - 6.19)
		Relative Body Weight	**Relative DFTD**
Year	**Relative Body Weight**	0.07 (0.03 - 0.13)	-0.38 (-0.75 - 0.10)
	Relative DFTD	-0.29 (-0.78 - 0.06)	8.98 (4.29 - 16.43)
Additive genetic	**Relative Body Weight**	0.11 (0.03 - 0.19)	-0.52 (-0.92 - -0.09)
	Relative DFTD	-0.27 (-0.49 - -0.05)	2.95 (1.36 - 4.81)
Permanent environment	**Relative Body Weight**	0.07 (0.01 - 0.13)	0.29 (-0.54 - 0.92)
	Relative DFTD	0.06 (-0.08 - 0.20)	0.82 (0.01 - 2.13)
Trap	**Relative Body Weight**	0.04 (0.01 - 0.07)	0.47 (-0.32 - 0.96)
	Relative DFTD	0.04 (-0.01 - 0.12)	0.28 (0.01 - 0.76)
Residual	**Relative Body Weight**	0.15 (0.13 - 0.18)	-0.12 (-0.23 - -0.002)
	Relative DFTD	-0.11 (-0.21 - -0.001)	5.31 (4.47 - 6.24)

824 **Figure S4.** Genetic correlations (COR_A), permanent environment correlation (COR_{PE}), year
825 correlation (COR_{Year}) and spatial correlation (COR_{TrapID}) between head width and body
826 weight, DFTD and head width and DFTD and body weight estimated from (a) models fit with
827 DFTD as a binary variable ("Original"), and (b) models fit with a relative measure of DFTD
828 (DFTD relative to the average prevalence of DFTD in the population, see methods for
829 details), which fit with gaussian errors ("Relative"). Covariance estimates can be found in
830 Table S3. Posterior median of estimates shown as point, with 75% CIs shown as heavy lines
831 and 95% CIs as lighter lines.

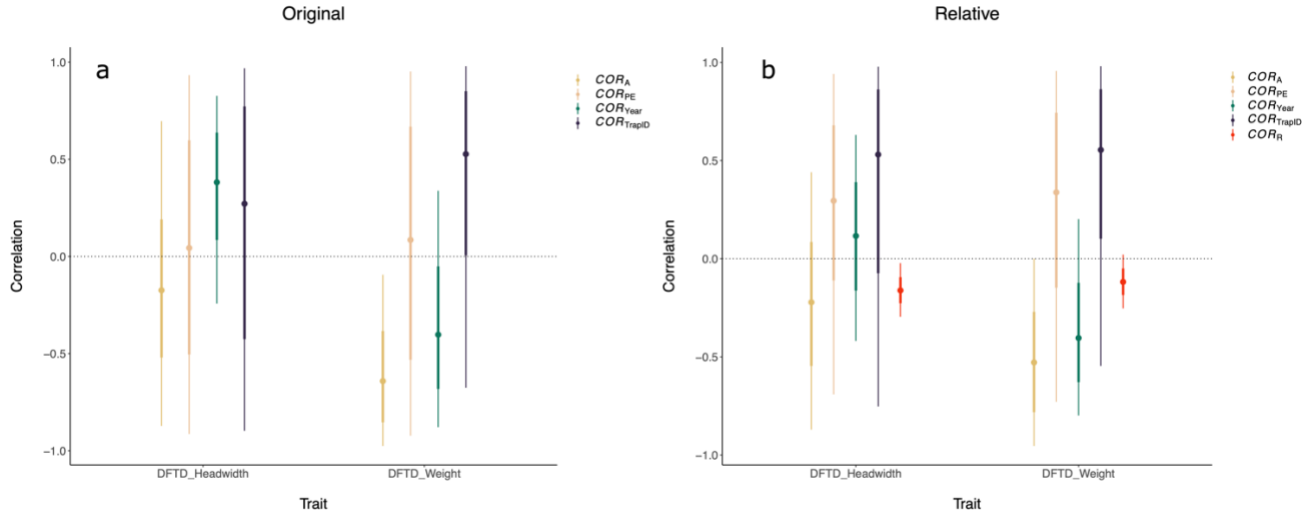

832

References

Ali, O. A., O'Rourke, S. M., Amish, S. J., Meek, M. H., Luikart, G., Jeffres, C., & Miller, M. R. (2016). RAD Capture (Rapture): Flexible and Efficient Sequence-Based Genotyping. *Genetics*, *202*(2), 389–400. https://doi.org/10.1534/genetics.115.183665

Altizer, S., Harvell, D., & Friedle, E. (2003). Rapid evolutionary dynamics and disease threats to biodiversity. *Trends in Ecology & Evolution*, *18*(11), 589–596. https://doi.org/10.1016/j.tree.2003.08.013

Bérénos, C., Ellis, P. A., Pilkington, J. G., & Pemberton, J. M. (2014). Estimating quantitative genetic parameters in wild populations: A comparison of pedigree and genomic approaches. *Molecular Ecology*, *23*(14), 3434–3451. https://doi.org/10.1111/mec.12827

Best, A., White, A., & Boots, M. (2008). Maintenance of host variation in tolerance to pathogens and parasites. *Proceedings of the National Academy of Sciences*, *105*(52), 20786–20791. https://doi.org/10.1073/pnas.0809558105

Boots, M., Best, A., Miller, M. R., & White, A. (2009). The role of ecological feedbacks in the evolution of host defence: What does theory tell us? *Philosophical Transactions of the Royal Society B: Biological Sciences*, *364*(1513), 27–36. https://doi.org/10.1098/rstb.2008.0160

Brüniche-Olsen, A., Burridge, C. P., Austin, J. J., & Jones, M. E. (2013). Disease induced changes in gene flow patterns among Tasmanian devil populations. *Biological Conservation*, *165*, 69–78. https://doi.org/10.1016/j.biocon.2013.05.014

Brüniche-Olsen, A., Jones, M. E., Austin, J. J., Burridge, C. P., & Holland, B. R. (2014). Extensive population decline in the Tasmanian devil predates European settlement

857 and devil facial tumour disease. *Biology Letters*, *10*(11), 20140619.
858 https://doi.org/10.1098/rsbl.2014.0619
859 Bulmer, M. G. (1971). The Effect of Selection on Genetic Variability. *The American*
860 *Naturalist*, *105*(943), 201–211. https://doi.org/10.1086/282718
861 Bürkner, P.-C. (2017). brms: An R package for Bayesian multilevel models using Stan. *Journal*
862 *of Statistical Software*, *80*(1), 1–28.
863 Bürkner, P.-C. (2021). Bayesian Item Response Modeling in R with brms and Stan. *Journal of*
864 *Statistical Software*, *100*(5), 1–54. https://doi.org/10.18637/jss.v100.i05
865 Catchen, J., Hohenlohe, P. A., Bassham, S., Amores, A., & Cresko, W. A. (2013). Stacks: An
866 analysis tool set for population genomics. *Molecular Ecology*, *22*(11), 3124–3140.
867 https://doi.org/10.1111/mec.12354
868 Charlesworth, D., & Willis, J. H. (2009). The genetics of inbreeding depression. *Nature*
869 *Reviews Genetics*, *10*(11), 783–796. https://doi.org/10.1038/nrg2664
870 Coltman, D. W., Pilkington, J., Kruuk, L. E. B., Wilson, K., & Pemberton, J. M. (2001). Positive
871 genetic correlation between parasite resistance and body size in a free-living
872 ungulate population. *Evolution*, *55*(10), 2116–2125. https://doi.org/10.1111/j.0014-
873 3820.2001.tb01326.x
874 Cristescu, R. H., Strickland, K., Schultz, A. J., Kruuk, L. E. B., de Villiers, D., & Frère, C. H.
875 (2022). Susceptibility to a sexually transmitted disease in a wild koala population
876 shows heritable genetic variance but no inbreeding depression. *Molecular Ecology*,
877 *31*(21), 5455–5467. https://doi.org/10.1111/mec.16676
878 Cunningham, C. X., Comte, S., McCallum, H., Hamilton, D. G., Hamede, R., Storfer, A.,
879 Hollings, T., Ruiz-Aravena, M., Kerlin, D. H., Brook, B. W., Hocking, G., & Jones, M. E.
880 (2021). Quantifying 25 years of disease-caused declines in Tasmanian devil

881 populations: Host density drives spatial pathogen spread. *Ecology Letters*, *24*(5),
882 958–969. https://doi.org/10.1111/ele.13703
883 Daszak, P., Cunningham, A., & Hyatt, A. D. (2000). Emerging Infectious Diseases of Wildlife—
884 Threats to Biodiversity and Human Health. *Science*, *287*(5452), 443–449.
885 https://doi.org/10.1126/science.287.5452.443
886 de Villemereuil, P., Schielzeth, H., Nakagawa, S., & Morrissey, M. (2016). General Methods
887 for Evolutionary Quantitative Genetic Inference from Generalized Mixed Models.
888 *Genetics*, *204*(3), 1281–1294. https://doi.org/10.1534/genetics.115.186536 %J
889 Genetics
890 DeRose, M. A., & Roff, D. A. (1999). A COMPARISON OF INBREEDING DEPRESSION IN LIFE-
891 HISTORY AND MORPHOLOGICAL TRAITS IN ANIMALS. *Evolution*, *53*(4), 1288–1292.
892 https://doi.org/10.1111/j.1558-5646.1999.tb04541.x
893 Epstein, B., Jones, M., Hamede, R., Hendricks, S., McCallum, H., Murchison, E. P., Schönfeld,
894 B., Wiench, C., Hohenlohe, P., & Storfer, A. (2016). Rapid evolutionary response to a
895 transmissible cancer in Tasmanian devils. *Nature Communications*, *7*(1), 12684.
896 https://doi.org/10.1038/ncomms12684
897 Falconer, D. S., & Mackay, T. F. C. (1996). Introduction to quantitative genetics. *Introduction*
898 *to Quantitative Genetics.*, *Ed. 4*.
899 Fisher, M. C., & Garner, T. W. J. (2020). Chytrid fungi and global amphibian declines. *Nature*
900 *Reviews Microbiology*, *18*(6), 332–343. https://doi.org/10.1038/s41579-020-0335-x
901 Fraik, A. K., Margres, M. J., Epstein, B., Barbosa, S., Jones, M., Hendricks, S., Schönfeld, B.,
902 Stahlke, A. R., Veillet, A., Hamede, R., McCallum, H., Lopez-Contreras, E., Kallinen, S.
903 J., Hohenlohe, P. A., Kelley, J. L., & Storfer, A. (2020). Disease swamps molecular
904 signatures of genetic-environmental associations to abiotic factors in Tasmanian

905 devil (Sarcophilus harrisii) populations. *Evolution*, *74*(7), 1392–1408.
906 https://doi.org/10.1111/evo.14023
907 Gervais, L., Perrier, C., Bernard, M., Merlet, J., Pemberton, J. M., Pujol, B., & Quéméré, E.
908 (2019). RAD-sequencing for estimating genomic relatedness matrix-based heritability
909 in the wild: A case study in roe deer. *Molecular Ecology Resources*, *19*(5), 1205–1217.
910 https://doi.org/10.1111/1755-0998.13031
911 Gienapp, P., Fior, S., Guillaume, F., Lasky, J. R., Sork, V. L., & Csilléry, K. (2017). Genomic
912 Quantitative Genetics to Study Evolution in the Wild. *Trends in Ecology & Evolution*,
913 *32*(12), 897–908. https://doi.org/10.1016/j.tree.2017.09.004
914 Gleeson, D. J., Blows, M. W., & Owens, I. P. (2005). Genetic covariance between indices of
915 body condition and immunocompetence in a passerine bird. *BMC Evolutionary*
916 *Biology*, *5*(1), 61. https://doi.org/10.1186/1471-2148-5-61
917 Golas, B. D., Goodell, B., & Webb, C. T. (2021). Host adaptation to novel pathogen
918 introduction: Predicting conditions that promote evolutionary rescue. *Ecology*
919 *Letters*, *24*(10), 2238–2255.
920 Gooley, R., Hogg, C. J., Belov, K., & Grueber, C. E. (2017). No evidence of inbreeding
921 depression in a Tasmanian devil insurance population despite significant variation in
922 inbreeding. *Scientific Reports*, *7*(1), 1830. https://doi.org/10.1038/s41598-017-
923 02000-y
924 Gooley, R. M., Hogg, C. J., Fox, S., Pemberton, D., Belov, K., & Grueber, C. E. (2020).
925 Inbreeding depression in one of the last DFTD-free wild populations of Tasmanian
926 devils. *PeerJ*, e9220. https://doi.org/10.7717/peerj.9220

927 Grossen, C., Guillaume, F., Keller, L. F., & Croll, D. (2020). Purging of highly deleterious
928 mutations through severe bottlenecks in Alpine ibex. *Nature Communications*, *11*(1),
929 1001. https://doi.org/10.1038/s41467-020-14803-1
930 Hajduk, G. K., Cockburn, A., Margraf, N., Osmond, H. L., Walling, C. A., & Kruuk, L. E. B.
931 (2018). Inbreeding, inbreeding depression, and infidelity in a cooperatively breeding
932 bird*. *Evolution*, *72*(7), 1500–1514. https://doi.org/10.1111/evo.13496
933 Hamede, R. K., Bashford, J., McCallum, H., & Jones, M. (2009). Contact networks in a wild
934 Tasmanian devil (Sarcophilus harrisii) population: Using social network analysis to
935 reveal seasonal variability in social behaviour and its implications for transmission of
936 devil facial tumour disease. *Ecology Letters*, *12*(11), 1147–1157.
937 https://doi.org/10.1111/j.1461-0248.2009.01370.x
938 Hamede, R. K., McCallum, H., & Jones, M. (2008). Seasonal, demographic and density-
939 related patterns of contact between Tasmanian devils (Sarcophilus harrisii):
940 Implications for transmission of devil facial tumour disease. *Austral Ecology*, *33*(5),
941 614–622. https://doi.org/10.1111/j.1442-9993.2007.01827.x
942 Hamede, R. K., McCallum, H., & Jones, M. (2013). Biting injuries and transmission of
943 Tasmanian devil facial tumour disease. *Journal of Animal Ecology*, *82*(1), 182–190.
944 https://doi.org/10.1111/j.1365-2656.2012.02025.x
945 Hamede, R. K., Owen, R., Siddle, H., Peck, S., Jones, M., Dujon, A. M., Giraudeau, M., Roche,
946 B., Ujvari, B., & Thomas, F. (2020). The ecology and evolution of wildlife cancers:
947 Applications for management and conservation. *Evolutionary Applications*, *13*(7),
948 1719–1732. https://doi.org/10.1111/eva.12948
949 Hamede, R. K., Pearse, A.-M., Swift, K., Barmuta, L. A., Murchison, E. P., & Jones, M. E.
950 (2015). Transmissible cancer in Tasmanian devils: Localized lineage replacement and

951 host population response. *Proceedings of the Royal Society B: Biological Sciences*,
952 *282*(1814), 20151468. https://doi.org/10.1098/rspb.2015.1468
953 Hamilton, D. G., Jones, M. E., Cameron, E. Z., Kerlin, D. H., McCallum, H., Storfer, A.,
954 Hohenlohe, P. A., & Hamede, R. K. (2020). Infectious disease and sickness behaviour:
955 Tumour progression affects interaction patterns and social network structure in wild
956 Tasmanian devils. *Proceedings of the Royal Society B: Biological Sciences*, *287*(1940),
957 20202454. https://doi.org/10.1098/rspb.2020.2454
958 Hamilton, D. G., Jones, M. E., Cameron, E. Z., McCallum, H., Storfer, A., Hohenlohe, P. A., &
959 Hamede, R. K. (2019). Rate of intersexual interactions affects injury likelihood in
960 Tasmanian devil contact networks. *Behavioral Ecology*, *30*(4), 1087–1095.
961 https://doi.org/10.1093/beheco/arz054
962 Hayward, A. D., Nussey, D. H., Wilson, A. J., Berenos, C., Pilkington, J. G., Watt, K. A.,
963 Pemberton, J. M., & Graham, A. L. (2014). Natural Selection on Individual Variation in
964 Tolerance of Gastrointestinal Nematode Infection. *PLOS Biology*, *12*(7), e1001917.
965 https://doi.org/10.1371/journal.pbio.1001917
966 Healy, K., Ezard, T. H. G., Jones, O. R., Salguero-Gómez, R., & Buckley, Y. M. (2019). Animal
967 life history is shaped by the pace of life and the distribution of age-specific mortality
968 and reproduction. *Nature Ecology & Evolution*, *3*(8), 1217–1224.
969 https://doi.org/10.1038/s41559-019-0938-7
970 Hedrick, P. W., & Garcia-Dorado, A. (2016). Understanding Inbreeding Depression, Purging,
971 and Genetic Rescue. *Trends in Ecology & Evolution*, *31*(12), 940–952.
972 https://doi.org/10.1016/j.tree.2016.09.005

973 Hedrick, P. W., & Kalinowski, S. T. (2000). Inbreeding Depression in Conservation Biology.
974 *Annual Review of Ecology and Systematics*, *31*(1), 139–162.
975 https://doi.org/10.1146/annurev.ecolsys.31.1.139
976 Herrera, J., & Nunn, C. L. (2019). Behavioural ecology and infectious disease: Implications for
977 conservation of biodiversity. *Philosophical Transactions of the Royal Society B:*
978 *Biological Sciences*, *374*(1781), 20180054. https://doi.org/10.1098/rstb.2018.0054
979 Hoffmann, A. A., Sgrò, C. M., & Kristensen, T. N. (2017). Revisiting Adaptive Potential,
980 Population Size, and Conservation. *Trends in Ecology & Evolution*, *32*(7), 506–517.
981 https://doi.org/10.1016/j.tree.2017.03.012
982 Hoffmann, C., Zimmermann, F., Biek, R., Kuehl, H., Nowak, K., Mundry, R., Agbor, A.,
983 Angedakin, S., Arandjelovic, M., Blankenburg, A., Brazolla, G., Corogenes, K., Couacy-
984 Hymann, E., Deschner, T., Dieguez, P., Dierks, K., Düx, A., Dupke, S., Eshuis, H., …
985 Leendertz, F. H. (2017). Persistent anthrax as a major driver of wildlife mortality in a
986 tropical rainforest. *Nature*, *548*(7665), 82–86. https://doi.org/10.1038/nature23309
987 Hoyt, J. R., Kilpatrick, A. M., & Langwig, K. E. (2021). Ecology and impacts of white-nose
988 syndrome on bats. *Nature Reviews Microbiology*, *19*(3), 196–210.
989 https://doi.org/10.1038/s41579-020-00493-5
990 Huisman, J. (2017). Pedigree reconstruction from SNP data: Parentage assignment, sibship
991 clustering and beyond. *Molecular Ecology Resources*, *17*(5), 1009–1024.
992 https://doi.org/10.1111/1755-0998.12665
993 Huisman, J., Kruuk, L. E. B., Ellis, P. A., Clutton-Brock, T., & Pemberton, J. M. (2016).
994 Inbreeding depression across the lifespan in a wild mammal population. *Proceedings*
995 *of the National Academy of Sciences*, *113*(13), 3585–3590.
996 https://doi.org/10.1073/pnas.1518046113

James, C, Pemberton, Josephine, Navarro, Pau, & Knott, Sara. (2023). Investigating pedigree- and SNP-associated components of heritability in a wild population of Soay sheep. *bioRxiv*, 2023.06.02.543397. https://doi.org/10.1101/2023.06.02.543397

Jones, M. E. (2023). Over-eruption in marsupial carnivore teeth: Compensation for a constraint. *Proceedings of the Royal Society B: Biological Sciences*, *290*(2013), 20230644. https://doi.org/10.1098/rspb.2023.0644

Jones, M. E., Cockburn, A., Hamede, R., Hawkins, C., Hesterman, H., Lachish, S., Mann, D., McCallum, H., & Pemberton, D. (2008). Life-history change in disease-ravaged Tasmanian devil populations. *Proceedings of the National Academy of Sciences*, *105*(29), 10023–10027. https://doi.org/10.1073/pnas.0711236105

Kirkpatrick, M., & Jarne, P. (2000). The Effects of a Bottleneck on Inbreeding Depression and the Genetic Load. *The American Naturalist*, *155*(2), 154–167. https://doi.org/10.1086/303312

Kruuk, L. E. B. (2004). Estimating genetic parameters in natural populations using the 'animal model'. *Proceedings of the Royal Society of London, Series B.*, *359*, 873–890.

Kruuk, L. E. B., & Hadfield, J. D. (2007). How to separate genetic and environmental causes of similarity between relatives. *Journal of Evolutionary Biology*, *20*(5), 1890–1903. https://doi.org/10.1111/j.1420-9101.2007.01377.x

Lachish, S., Jones, M., & McCallum, H. (2007). The Impact of Disease on the Survival and Population Growth Rate of the Tasmanian Devil. *Journal of Animal Ecology*, *76*(5), 926–936. JSTOR.

Lachish, S., McCallum, H., & Jones, M. (2009). Demography, Disease and the Devil: Life-History Changes in a Disease-Affected Population of Tasmanian Devils (Sarcophilus harrisii). *Journal of Animal Ecology*, *78*(2), 427–436. JSTOR.

1021 Laikre, L., & Ryman, N. (1991). Inbreeding Depression in a Captive Wolf (Canis lupus)
1022 Population. *Conservation Biology*, *5*(1), 33–40. https://doi.org/10.1111/j.1523-
1023 1739.1991.tb00385.x
1024 Lande, R., & Arnold, S. J. (1983). The Measurement of Selection on Correlated Characters.
1025 *Evolution*, *37*(6), 1210–1226. JSTOR. https://doi.org/10.2307/2408842
1026 Margres, M. J., Jones, M. E., Epstein, B., Kerlin, D. H., Comte, S., Fox, S., Fraik, A. K.,
1027 Hendricks, S. A., Huxtable, S., Lachish, S., Lazenby, B., O'Rourke, S. M., Stahlke, A. R.,
1028 Wiench, C. G., Hamede, R., Schönfeld, B., McCallum, H., Miller, M. R., Hohenlohe, P.
1029 A., & Storfer, A. (2018). Large-effect loci affect survival in Tasmanian devils
1030 (Sarcophilus harrisii) infected with a transmissible cancer. *Molecular Ecology*, *27*(21),
1031 4189–4199. https://doi.org/10.1111/mec.14853
1032 Marjamäki, P. H., Dugdale, H. L., Delahay, R., McDonald, R. A., & Wilson, A. J. (2021).
1033 Genetic, social and maternal contributions to Mycobacterium bovis infection status
1034 in European badgers (Meles meles). *Journal of Evolutionary Biology*, *34*(4), 695–709.
1035 Martin, A. M., Cassirer, E. F., Waits, L. P., Plowright, R. K., Cross, P. C., & Andrews, K. R.
1036 (2021). Genomic association with pathogen carriage in bighorn sheep (Ovis
1037 canadensis). *Ecology and Evolution*, *11*(6), 2488–2502.
1038 McCallum, H. (2008). Tasmanian devil facial tumour disease: Lessons for conservation
1039 biology. *Trends in Ecology & Evolution*, *23*(11), 631–637.
1040 https://doi.org/10.1016/j.tree.2008.07.001
1041 McCallum, H., Tompkins, D. M., Jones, M., Lachish, S., Marvanek, S., Lazenby, B., Hocking,
1042 G., Wiersma, J., & Hawkins, C. E. (2007). Distribution and Impacts of Tasmanian Devil
1043 Facial Tumor Disease. *EcoHealth*, *4*(3), 318–325. https://doi.org/10.1007/s10393-
1044 007-0118-0

1045 Medzhitov, R., Schneider, D. S., & Soares, M. P. (2012). Disease Tolerance as a Defense
1046 Strategy. *Science*, *335*(6071), 936–941. https://doi.org/10.1126/science.1214935
1047 Murchison, E. P., Schulz-Trieglaff, O. B., Ning, Z., Alexandrov, L. B., Bauer, M. J., Fu, B., Hims,
1048 M., Ding, Z., Ivakhno, S., Stewart, C., Ng, B. L., Wong, W., Aken, B., White, S., Alsop,
1049 A., Becq, J., Bignell, G. R., Cheetham, R. K., Cheng, W., … Stratton, M. R. (2012).
1050 Genome Sequencing and Analysis of the Tasmanian Devil and Its Transmissible
1051 Cancer. *Cell*, *148*(4), 780–791. https://doi.org/10.1016/j.cell.2011.11.065
1052 Murchison, E. P., Tovar, C., Hsu, A., Bender, H. S., Kheradpour, P., Rebbeck, C. A., Obendorf,
1053 D., Conlan, C., Bahlo, M., Blizzard, C. A., Pyecroft, S., Kreiss, A., Kellis, M., Stark, A.,
1054 Harkins, T. T., Graves, J. A. M., Woods, G. M., Hannon, G. J., & Papenfuss, A. T.
1055 (2010). The Tasmanian Devil Transcriptome Reveals Schwann Cell Origins of a
1056 Clonally Transmissible Cancer. *Science*, *327*(5961), 84–87.
1057 https://doi.org/10.1126/science.1180616
1058 Nielsen, J. F., English, S., Goodall-Copestake, W. P., Wang, J., Walling, C. A., Bateman, A. W.,
1059 Flower, T. P., Sutcliffe, R. L., Samson, J., Thavarajah, N. K., Kruuk, L. E. B., Clutton-
1060 Brock, T. H., & Pemberton, J. M. (2012). Inbreeding and inbreeding depression of
1061 early life traits in a cooperative mammal. *Molecular Ecology*, *21*(11), 2788–2804.
1062 https://doi.org/10.1111/j.1365-294X.2012.05565.x
1063 O'Grady, J. J., Brook, B. W., Reed, D. H., Ballou, J. D., Tonkyn, D. W., & Frankham, R. (2006).
1064 Realistic levels of inbreeding depression strongly affect extinction risk in wild
1065 populations. *Biological Conservation*, *133*(1), 42–51.
1066 https://doi.org/10.1016/j.biocon.2006.05.016
1067 Patton, A. H., Lawrance, M. F., Margres, M. J., Kozakiewicz, C. P., Hamede, R., Ruiz-Aravena,
1068 M., Hamilton, D. G., Comte, S., Ricci, L. E., Taylor, R. L., Stadler, T., Leaché, A.,

McCallum, H., Jones, M. E., Hohenlohe, P. A., & Storfer, A. (2020). A transmissible cancer shifts from emergence to endemism in Tasmanian devils. *Science*, *370*(6522), eabb9772. https://doi.org/10.1126/science.abb9772

Price, G. R. (1970). Selection and covariance. *Nature*, *227*, 520–521. CABDirect. https://doi.org/10.1038/227520a0

Pye, R., Hamede, R., Siddle, H. V., Caldwell, A., Knowles, G. W., Swift, K., Kreiss, A., Jones, M. E., Lyons, A. B., & Woods, G. M. (2016). Demonstration of immune responses against devil facial tumour disease in wild Tasmanian devils. *Biology Letters*, *12*(10), 20160553. https://doi.org/10.1098/rsbl.2016.0553

Rarberg, L., & Stjernman, M. (2003). Natural selection on immune responsiveness in blue tits Parus caeruleus. *Evolution*, *57*(7), 1670–1678. https://doi.org/10.1111/j.0014-3820.2003.tb00372.x

Reid, J. M., Arcese, P., & Keller, L. F. (2003). Inbreeding depresses immune response in song sparrows (Melospiza melodia): Direct and inter–generational effects. *Proceedings of the Royal Society of London. Series B: Biological Sciences*, *270*(1529), 2151–2157. https://doi.org/10.1098/rspb.2003.2480

Rigby, M. C., Hechinger, R. F., & Stevens, L. (2002). Why should parasite resistance be costly? *Trends in Parasitology*, *18*(3), 116–120. https://doi.org/10.1016/S1471-4922(01)02203-6

Robertson, A., & Lewontin, R. (1968). Population biology and evolution. *The Spectrum of Genetic Variation. Syracuse Univ. Press, New York*, 5–16.

Rogalski, M. A., Gowler, C. D., Shaw, C. L., Hufbauer, R. A., & Duffy, M. A. (2017). Human drivers of ecological and evolutionary dynamics in emerging and disappearing

infectious disease systems. *Philosophical Transactions of the Royal Society B: Biological Sciences*, *372*(1712), 20160043. https://doi.org/10.1098/rstb.2016.0043

Ross-Gillespie, A., O'Riain, M. J., & Keller, L. F. (2007). VIRAL EPIZOOTIC REVEALS INBREEDING DEPRESSION IN A HABITUALLY INBREEDING MAMMAL. *Evolution*, *61*(9), 2268–2273. https://doi.org/10.1111/j.1558-5646.2007.00177.x

Sánchez, C. A., Becker, D. J., Teitelbaum, C. S., Barriga, P., Brown, L. M., Majewska, A. A., Hall, R. J., & Altizer, S. (2018). On the relationship between body condition and parasite infection in wildlife: A review and meta-analysis. *Ecology Letters*, *21*(12), 1869–1884. https://doi.org/10.1111/ele.13160

Schrag, S. J., & Wiener, P. (1995). Emerging infectious disease: What are the relative roles of ecology and evolution? *Trends in Ecology & Evolution*, *10*(8), 319–324. https://doi.org/10.1016/S0169-5347(00)89118-1

Silk, M. J., & Hodgson, D. J. (2021). Life history and population regulation shape demographic competence and influence the maintenance of endemic disease. *Nature Ecology & Evolution*, *5*(1), 82–91. https://doi.org/10.1038/s41559-020-01333-8

Spielman, D., Brook, B. W., Briscoe, D. A., & Frankham, R. (2004). Does Inbreeding and Loss of Genetic Diversity Decrease Disease Resistance? *Conservation Genetics*, *5*(4), 439–448. https://doi.org/10.1023/B:COGE.0000041030.76598.cd

Stahlke, A. R., Epstein, B., Barbosa, S., Margres, M. J., Patton, A. H., Hendricks, S. A., Veillet, A., Fraik, A. K., Schönfeld, B., McCallum, H. I., Hamede, R., Jones, M. E., Storfer, A., & Hohenlohe, P. A. (2021). Contemporary and historical selection in Tasmanian devils (Sarcophilus harrisii) support novel, polygenic response to transmissible cancer.

Proceedings of the Royal Society B: Biological Sciences, *288*(1951), 20210577. https://doi.org/10.1098/rspb.2021.0577

Stammnitz, M. R., Gori, K., Kwon, Y. M., Harry, E., Martin, F. J., Billis, K., Cheng, Y., Baez-Ortega, A., Chow, W., Comte, S., Eggertsson, H., Fox, S., Hamede, R., Jones, M., Lazenby, B., Peck, S., Pye, R., Quail, M. A., Swift, K., … Murchison, E. P. (2023). The evolution of two transmissible cancers in Tasmanian devils. *Science*, *380*(6642), 283–293. https://doi.org/10.1126/science.abq6453

Trinkel, M., Cooper, D., Packer, C., & Slotow, R. (2011). INBREEDING DEPRESSION INCREASES SUSCEPTIBILITY TO BOVINE TUBERCULOSIS IN LIONS: AN EXPERIMENTAL TEST USING AN INBRED–OUTBRED CONTRAST THROUGH TRANSLOCATION. *Journal of Wildlife Diseases*, *47*(3), 494–500. https://doi.org/10.7589/0090-3558-47.3.494

Valenzuela-Sánchez, A., Wilber, M. Q., Canessa, S., Bacigalupe, L. D., Muths, E., Schmidt, B. R., Cunningham, A. A., Ozgul, A., Johnson, P. T. J., & Cayuela, H. (2021). Why disease ecology needs life-history theory: A host perspective. *Ecology Letters*, *24*(4), 876–890. https://doi.org/10.1111/ele.13681

Walsh, B., & Lynch, M. (2018). *Evolution and selection of quantitative traits*. Oxford University Press.

Wang, J. (2010). coancestry: A program for simulating, estimating and analysing relatedness and inbreeding coefficients. *Molecular Ecology Resources*, *11*(1), 141–145. https://doi.org/10.1111/j.1755-0998.2010.02885.x

Wilson, A. J., Coltman, D. W., Pemberton, J. M., Overall, A. D. J., Byrne, K. A., & Kruuk, L. E. B. (2005). Maternal genetic effects set the potential for evolution in a free-living vertebrate population. *Journal of Evolutionary Biology*, *18*(2), 405–414. https://doi.org/10.1111/j.1420-9101.2004.00824.x

Wilson, A. J., Réale, D., Clements, M. N., Morrissey, M. M., Postma, E., Walling, C. A., Kruuk, L. E. B., & Nussey, D. H. (2010). An ecologist's guide to the animal model. *Journal of Animal Ecology*, *79*(1), 13–26. https://doi.org/10.1111/j.1365-2656.2009.01639.x

Yang, J., Lee, S. H., Goddard, M. E., & Visscher, P. M. (2011). GCTA: a tool for genome-wide complex trait analysis. *American Journal of Human Genetics*, *88*(1), 76–82. https://doi.org/10.1016/j.ajhg.2010.11.011

Zaitlen, N., Kraft, P., Patterson, N., Pasaniuc, B., Bhatia, G., Pollack, S., & Price, A. L. (2013). Using Extended Genealogy to Estimate Components of Heritability for 23 Quantitative and Dichotomous Traits. *PLOS Genetics*, *9*(5), e1003520. https://doi.org/10.1371/journal.pgen.1003520